Digital Multi-Carrier Spread Spectrum Versus Direct Sequence Spread Spectrum for Resistance to Jamming and Multipath

Shengli Zhou, *Student Member, IEEE*, Georgios B. Giannakis, *Fellow, IEEE*, and Ananthram Swami, *Senior Member, IEEE*

***Abstract*—We compare single user digital multi-carrier spread spectrum (MC-SS) modulation with direct sequence (DS) SS (with a modified implementation) in the presence of narrowband interference (NBI) and multipath fading. We derive closed-form expressions for the symbol error probability for both the linear MMSE receiver as well as the conventional matched-filter receiver under different scenarios: additive white Gaussian noise (AWGN) channel with NBI, multipath channel with or without NBI. We show that DS-SS can achieve the same performance as MC-SS if the spreading code is carefully designed to have perfect periodic autocorrelation function (PACF). On the other hand, MC-SS is more robust to narrowband interference and multipath fading than is DS-SS with the widely used spreading codes that do not possess perfect PACF. Our analysis reveals that the performance improvement of MC-SS is precisely due to the implicit construction of an equivalent spreading code having nonconstant amplitude but possessing perfect periodic autocorrelation.**

***Index Terms*—Direct-sequence, frequency-selective fading, multi-carrier, multipath, narrowband interference, periodic autocorrelation function, spread spectrum.**

I. Introduction

THE increasing interest and applications of direct sequence spread spectrum (DS-SS) technology stem from its robustness to fading, its anti-interference capability, and the potential for (even uncoordinated) multiple access [29]. With a wide bandwidth, and thus a short chip period, multiple paths can be resolved with DS-SS transmissions and a RAKE receiver can be used to mitigate fading and improve system performance [21]. De-spreading the received signal with the pre-determined code sequence, attenuates the narrowband interference, which may be due to intentional jamming or narrowband communication links that co-exist with wide band transmissions [17]. The anti-interference capability is measured by the amount of attenuation, and depends on the system's processing gain [29].

Paper approved by S. L. Miller, the Editor for Spread Spectrum of the IEEE Communications Society. Manuscript received October 17, 2000; revised July 15, 2001. This work was supported by ARL under Grant DAAL01-98-Q-0648 and by National Sceince Foundation under NSF Wireless Initiative Grant 99-79443. This paper was presented in part at the SPIE Digital Wireless Communications III, Orlando, FL, April 16–20, 2001, and at the International Conference on Acoustics, Speech, and Signal Processing (ICASSP), Salt Lake City, UT, May 7–11, 2001.

S. Zhou and G. B. Giannakis are with the Department of Electrical and Computer Engineering, University of Minnesota, Minneapolis, MN 55455 USA (e-mail: szhou@ece.umn.edu; georgios@ece.umn.edu).

A. Swami is with the Army Research Laboratory, AMSRL-CI-CN, Adelphi, MD 20783 USA (e-mail: aswami@arl.army.mil).

Publisher Item Identifier S 0090-6778(02)03508-0.

An alternative to DS-SS signaling, called frequency-diversity spread spectrum (FD-SS), was recently proposed and shown to be more resistant than DS-SS to narrowband and partial band interference (NBI/PBI) [14]. FD-SS, with disjoint frequency support for each subcarrier, is, in fact, the analog counterpart of digital OFDM spread spectrum technique [23], [24] and the underlying multicarrier spread spectrum (MC-SS) approach for multicarrier (MC) CDMA with overlapping subcarriers [27]. By exploiting multiple carriers and a narrowband DS waveform on each subcarrier, it has been shown that multicarrier DS CDMA outperforms single carrier CDMA for wideband transmissions in the presence of narrowband interference [16]; results for partial-time jamming may be found in [5].

Although most existing works rely on analog carrier modulations, digital implementations through FFT's are also available [1], [14]. Thanks to the rapid development of digital devices and digital signal processing (DSP) technologies, the digital-to-analog (D/A) and analog-to-digital (A/D) converters are being pushed closer to the transceiver's end. A unifying digital implementation framework of many existing schemes has been developed [10], [26], which includes MC-CDMA [27] and MC-DS-CDMA [16] as special cases.

In this paper, we focus on the *single user* scenario where the narrowband signals are spread over a much wider bandwidth to combat narrowband interference and multipath fading. Starting from a discrete-time equivalent model, we investigate the performance of digital MC-SS, and compare it with DS-SS. We show that DS-SS can achieve the same performance as MC-SS, if the spreading code is carefully designed with perfect periodic autocorrelation function (PACF). On the other hand, MC-SS is more robust to narrowband interference and multipath fading than is DS-SS with commonly used spreading codes not having perfect PACF. We show that the performance improvement of MC-SS is precisely due to the implicit construction of an equivalent spreading code having nonconstant amplitude but possessing perfect periodic autocorrelation. The main contributions of this paper are the novel results on performance analysis of digital MC-SS and DS-SS in the presence of jamming and multipath.

The rest of this paper is organized as follows. The discrete-time system model is introduced in Section II. MC-SS and DS-SS are then compared under various conditions: additive white Gaussian noise (AWGN) channels with narrowband and partial band interference (NBI/PBI) in Section III, frequency-selective multipath channels in Section IV, and mul-

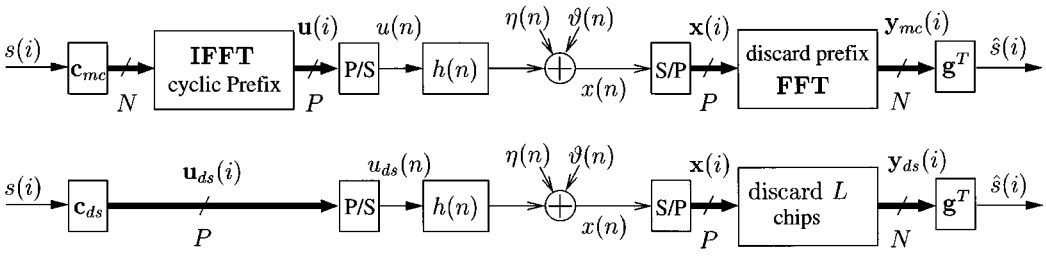

Fig. 1. Discrete-time equivalent baseband model for MC-SS (upper part) and DS-SS (lower part).

tipath fading channels with NBI/PBI in Section V. Discussion and conclusions are collected in Section VI.

II. Unifying Digital MC-SS and DS-SS Models

The diagram in the upper part of Fig. 1 describes the discrete-time baseband equivalent model of an MC-SS system, where signals, codes, and channels are represented by samples of their complex envelopes taken at the chip rate. The length-N symbol periodic digital spreading code $\mathbf{c}_{\rm mc} := [c_{\rm mc}(0),\ldots,c_{\rm mc}(N-1)]^T$ spreads the ith information symbol $s(i)$. We assume in this paper that the spreading sequence has unit amplitude, e.g., taking binary (± 1) values, or any complex number on the unit circle. The resulting $N\times 1$ vector $\mathbf{c}_{\rm mc}s(i)$ is mapped into a $P\times 1$ vector, $\mathbf{u}(i) := [u(iP), u(iP+1),\ldots,u(iP+P-1)]^T$ as follows. The length-N IFFT of $\mathbf{c}_{\rm mc}s(i)$ is evaluated, and the last $P-N$ elements are replicated at the front to form the cyclic prefix (CP) as in conventional OFDM [1].

Let $\mathbf{I}_{\rm cp}$ denote the last $P-N$ rows of the $N\times N$ identity matrix $\mathbf{I}_N$, and let $\mathbf{F}_N$ be the $N\times N$ FFT matrix with (m,n)th entry $\left(1/\sqrt{N}\right)\exp(-j2\pi mn/N)$. Let $\mathbf{T}_{\rm cp} := \left[\mathbf{I}_{\rm cp}^T, \mathbf{I}_N^T\right]^T$ denote the $P\times N$ transmit-matrix, and $\mathbf{F}_N^{\mathcal{H}}$ denote the IFFT matrix, where $^{\mathcal{H}}$ denotes Hermitian transpose. Cyclic prefix insertion on a vector is accomplished by left multiplying it with $\mathbf{T}_{\rm cp}$, and the IFFT is obtained through multiplication by $\mathbf{F}_N^{\mathcal{H}}$. Hence, the ith transmitted block can be written as $\mathbf{u}(i) = \mathbf{T}_{\rm cp}\mathbf{F}_N^{\mathcal{H}}\mathbf{c}_{\rm mc}s(i)$.

The block $\mathbf{u}(i)$ is converted from parallel to serial (P/S), and the resulting sequence $u(n)$ is pulse shaped to obtain the continuous time signal $u_c(t) = \sum_{n=-\infty}^{\infty} u(n)\varphi(t-nT_c)$, where T_c is the chip period, and $\varphi(t)$ is the chip pulse. The subscript c in $u_c(t)$ (and later in $\eta_c(t)$ and $\vartheta_c(t)$) is a mnemonic for continuous-time. The transmitted signal[1] $u_c(t)$ propagates through a (possibly *unknown*) dispersive channel $h_c(t)$, and is filtered by the receive filter $\bar{\varphi}(t)$, that is matched to $\varphi(t)$. We suppose carrier synchronization has been performed with no errors. Let $\Gamma_{\varphi\bar{\varphi}}(t)$ denote the convolution of transmit- with receive-filters; by design, its spectrum has Nyquist characteristics, and bandwidth $B \geq 1/(2T_c)$. Let $\star$ denote convolution. Then $h(l) := (\varphi\star h_c\star\bar{\varphi})(t)|_{t=lT_c} = \int_{-\infty}^{\infty} h_c(\tau)\Gamma_{\varphi\bar{\varphi}}(lT_c-\tau)d\tau$ is the equivalent discrete time channel impulse response which includes frequency-selective multipath propagation as well as transmit–receive filter effects. The channel order is L, i.e., $h(l)=0,\ \forall\, l\notin[0,L]$; L is the maximum number of chips affected by the multipath delay-spread (with $\tau_{\max}$ denoting the maximum delay spread, $L\approx\lceil\tau_{\max}/T_c\rceil$; see [21, p. 797]).

[1]There is no carrier since we are dealing with the baseband equivalent model.

Usually, the spreading length N and the channel order L satisfy $N>L$ (see also [16], [24], [27]). In the presence of additive Gaussian noise (AGN) $\eta_c(t)$ and NBI $\vartheta_c(t)$, the received signal, sampled at the chip rate, can be written as

$$\begin{aligned} x(n) =& h(n)\star u(n)+\eta(n)+\vartheta(n)\\ =&\sum_{l=0}^{L} h(l)u(n-l)+\eta(n)+\vartheta(n) \end{aligned} \tag{1}$$

where $\eta(n)=(\eta_c\star\bar{\varphi})(t)|_{t=nT_c}$, $\vartheta(n)=(\vartheta_c\star\bar{\varphi})(t)|_{t=nT_c}$ are filtered AGN and NBI, respectively. Because $\bar{\varphi}(t)$ has Nyquist characteristics, if $\eta_c(t)$ is white, so is $\eta(n)$.

To avoid intersymbol interference (ISI), the CP length should be larger than the channel order: $P-N\geq L$. To avoid bandwidth overexpansion, we choose the smallest block length: **As0)**: *The transmitted block length is* $P=N+L$.

To convert (1) from a serial to a convenient matrix-vector form, we define the $P\times 1$ vector: $\mathbf{x}(i) := [x(iP), x(iP+1),\ldots,x(iP+P-1)]^T$ and likewise for $\boldsymbol{\eta}(i)$ and $\boldsymbol{\vartheta}(i)$; the $P\times P$ Toeplitz channel matrices $\mathbf{H}_0$, $\mathbf{H}_1$ have (k,l)th entries $h(k-l)$ and $h(k-l+P)$, respectively. Since $h(l)=0,\ \forall\, l\notin[0,L]$, and $P=N+L$ under As0), we can write (1) as

$$\mathbf{x}(i)=\mathbf{H}_0\mathbf{u}(i)+\mathbf{H}_1\mathbf{u}(i-1)+\boldsymbol{\eta}(i)+\boldsymbol{\vartheta}(i) \tag{2}$$

where the second term in the right hand side represents interblock interference (IBI).

At the receiver end, the CP of length $P-N$ is removed first, and an FFT is performed on the remaining $N\times 1$ vector. In matrix form, this is accomplished with the receive-matrix $\mathbf{R}_{\rm cp} := [\mathbf{0}_{N\times(P-N)}, \mathbf{I}_N]$ which removes the first $P-N$ entries of a $P\times 1$ vector when the product $\mathbf{R}_{\rm cp}\mathbf{x}(i)$ is formed. According to As0), $\mathbf{R}_{\rm cp}\mathbf{H}_1=\mathbf{0}$ indicating that IBI (and thus ISI) is eliminated. For ease of notation, we define the truncated composite noise vector as

$$\bar{\mathbf{w}}(i) := \mathbf{R}_{\rm cp}\left[\boldsymbol{\eta}(i)+\boldsymbol{\vartheta}(i)\right]. \tag{3}$$

IBI removal, together with (3), allows one to express the FFT output of a digital multicarrier (mc) system as:

$$\begin{aligned} \mathbf{y}_{\rm mc}(i) =& \mathbf{F}_N\mathbf{R}_{\rm cp}\mathbf{x}(i)=\mathbf{F}_N\mathbf{R}_{\rm cp}\mathbf{H}_0\mathbf{u}(i)+\mathbf{F}_N\bar{\mathbf{w}}(i),\\ =&\mathbf{F}_N\mathbf{R}_{\rm cp}\mathbf{H}_0\mathbf{T}_{\rm cp}\mathbf{F}_N^{\mathcal{H}}\mathbf{c}_{\rm mc}s(i)+\mathbf{F}_N\bar{\mathbf{w}}(i),\\ =&\mathbf{F}_N\tilde{\mathbf{H}}\mathbf{F}_N^{\mathcal{H}}\mathbf{c}_{\rm mc}s(i)+\mathbf{F}_N\bar{\mathbf{w}}(i) \end{aligned} \tag{4}$$

where $\tilde{\mathbf{H}}=\mathbf{R}_{\rm cp}\mathbf{H}_0\mathbf{T}_{\rm cp}$ is the overall channel matrix. We verify by direct substitution that $\tilde{\mathbf{H}}$ is an $N\times N$ circulant matrix with (k,l)th entry given by $h((k-l)\bmod N)$. Because (I)FFT's diagonalize circulant matrices, the circulant matrix $\tilde{\mathbf{H}}$ can be decomposed as $\tilde{\mathbf{H}}=\mathbf{F}_N^{\mathcal{H}}\mathbf{D}(\tilde{\mathbf{h}})\mathbf{F}_N$, where

$\tilde{\mathbf{h}} := \left[H(e^{j0}), H\left(e^{j(2\pi/N)}\right), \ldots, H\left(e^{j(2\pi/N)(N-1)}\right)\right]^T$ with entries the channel frequency response $H(z) = \sum_{l=0}^{L} h(l)z^{-l}$ evaluated at the subcarriers $z_k = \exp(j2\pi k/N)$, and $\mathbf{D}(\tilde{\mathbf{h}}) := \text{diag}(\tilde{\mathbf{h}})$ denotes a diagonal matrix with the (i,i)th entry being the ith element of the vector $\tilde{\mathbf{h}}$; further details may be found in [26]. Therefore, we can rewrite (4) as

$$\mathbf{y}_{\text{mc}}(i) = \mathbf{D}(\tilde{\mathbf{h}})\mathbf{c}_{\text{mc}}s(i) + \mathbf{F}_N\bar{\mathbf{w}}(i). \tag{5}$$

With the matrix $\mathbf{D}(\mathbf{c}_{\text{mc}}) := \text{diag}(\mathbf{c}_{\text{mc}})$, we verify that $\mathbf{D}(\tilde{\mathbf{h}})\mathbf{c}_{\text{mc}} = \mathbf{D}(\mathbf{c}_{\text{mc}})\tilde{\mathbf{h}}$, and rewrite (5) as

$$\begin{aligned}\mathbf{y}_{\text{mc}}(i) =& \mathbf{D}(\mathbf{c}_{\text{mc}})\tilde{\mathbf{h}}s(i) + \mathbf{F}_N\bar{\mathbf{w}}(i)\\ =& \mathbf{D}(\mathbf{c}_{\text{mc}})\mathbf{V}\mathbf{h}s(i) + \mathbf{F}_N\bar{\mathbf{w}}(i)\end{aligned} \tag{6}$$

where $\mathbf{V}$ is a $N \times (L+1)$ Vandermonde matrix formed by the first $L+1$ columns of $\sqrt{N}\mathbf{F}_N$, $\mathbf{h} := [h(0), \ldots, h(L)]^T$, and $\tilde{\mathbf{h}} = \mathbf{V}\mathbf{h}$ represents a scalar FFT operation in matrix form.

Our primary goal is to compare the ability of MC-SS and DS-SS to combat NBI/PBI and multipath fading; therefore, we now describe the discrete time baseband model of DS-SS that is depicted in the lower part of Fig. 1.

Without FFT and CP insertion at the transmitter, the transmitted block in DS-SS is $\mathbf{u}_{\text{ds}}(i) = \mathbf{c}_{\text{ds}}s(i)$, where $\mathbf{c}_{\text{ds}} := [c_{\text{ds}}(0), c_{\text{ds}}(1), \ldots, c_{\text{ds}}(P-1)]^T$ is a $P \times 1$ vector having the same block length as the MC-SS system (the upper part of Fig. 1). Replacing $\mathbf{u}(i)$ in (2) by $\mathbf{u}_{\text{ds}}(i)$, and with $\mathbf{R}_{\text{cp}}$ eliminating IBI as in (4), we arrive at (see Remark 1 for more on this)

$$\mathbf{y}_{\text{ds}}(i) = \mathbf{R}_{\text{cp}}\mathbf{H}_0\mathbf{c}_{\text{ds}}s(i) + \bar{\mathbf{w}}(i). \tag{7}$$

Because $\mathbf{H}_0\mathbf{c}_{\text{ds}}$ represents in matrix-vector form the linear convolution between $\mathbf{h}$ and $\mathbf{c}_{\text{ds}}$, we can commute $\mathbf{h}$ and $\mathbf{c}_{\text{ds}}$ to obtain $\mathbf{H}_0\mathbf{c}_{\text{ds}} = \mathbf{C}_{\text{ds}}\mathbf{h}$, with $\mathbf{C}_{\text{ds}}$ denoting a $P \times (L+1)$ Toeplitz matrix with first column $\mathbf{c}_{\text{ds}}$ and first row $[c_{\text{ds}}(0), 0, \ldots, 0]$. Let us now define the truncated $N \times 1$ code vector for DS-SS as $\bar{\mathbf{c}}_{\text{ds}} := \mathbf{R}_{\text{cp}}\mathbf{c}_{\text{ds}}$. Multiplying $\mathbf{R}_{\text{cp}}$ with $\mathbf{C}_{\text{ds}}$ yields a truncated $N \times (L+1)$ Toeplitz matrix $\bar{\mathbf{C}}_{\text{ds}}$ with first column $\bar{\mathbf{c}}_{\text{ds}}$ and first row $[c_{\text{ds}}(L), \ldots, c_{\text{ds}}(0)]$. Therefore, we can rewrite (7) as:

$$\mathbf{y}_{\text{ds}}(i) = \bar{\mathbf{C}}_{\text{ds}}\mathbf{h}s(i) + \bar{\mathbf{w}}(i). \tag{8}$$

Comparing (6) with (8), we *unify* MC-SS and DS-SS in the following equivalent model:

$$\mathbf{y}(i) = \mathbf{C}\mathbf{h}s(i) + \mathbf{w}(i) = \mathbf{c}s(i) + \mathbf{w}(i) \tag{9}$$

where $\mathbf{c} := \mathbf{C}\mathbf{h}$ denotes the equivalent signature code vector after channel convolution and receiver processing. For convenience, we list the corresponding vectors in (9) for MC-SS as

$$\mathbf{y}(i) = \mathbf{y}_{\text{mc}}(i), \quad \mathbf{c} = \mathbf{D}(\mathbf{c}_{\text{mc}})\mathbf{V}\mathbf{h}, \quad \mathbf{w}(i) = \mathbf{F}_N\bar{\mathbf{w}}(i) \tag{10}$$

and for DS-SS as

$$\mathbf{y}(i) = \mathbf{y}_{\text{ds}}(i), \quad \mathbf{c} = \bar{\mathbf{C}}_{\text{ds}}\mathbf{h}, \quad \mathbf{w}(i) = \bar{\mathbf{w}}(i). \tag{11}$$

Relying on the unifying model (9), we will first find the linear MMSE receiver in addition to the conventional matched filter (MF), and then illustrate the differences between MC-SS and DS-SS under different scenarios in Sections III–VI.

If the noise $\mathbf{w}(i)$ in (9) is white, the optimum (in the ML sense) linear processor is the matched filter (or RAKE receiver) that is given by $\mathbf{g}_{\text{mf}}^T := \mathbf{c}^{\mathcal{H}}$. Define $\sigma_s^2 := E\left\{s(i)s^{\mathcal{H}}(i)\right\}$ and $\mathbf{R}_{ww} := E\left\{\mathbf{w}(i)\mathbf{w}^{\mathcal{H}}(i)\right\}$. The corresponding SNR at the MF output is thus

$$\text{SNR}_{\text{mf}} = \frac{E\left\{\left|\mathbf{g}_{\text{mf}}^T\mathbf{c}s\right|^2\right\}}{E\left\{\left|\mathbf{g}_{\text{mf}}^T\mathbf{w}\right|^2\right\}} = \frac{\sigma_s^2|\mathbf{c}^{\mathcal{H}}\mathbf{c}|^2}{\mathbf{c}^{\mathcal{H}}\mathbf{R}_{ww}\mathbf{c}}. \tag{12}$$

Due to the presence of NBI/PBI, the noise $\mathbf{w}(i)$ is colored which renders the MF suboptimal and motivates the use of minimum mean-square error (MMSE) receivers. Based on (9), the linear MMSE receiver $\mathbf{g}_{\text{mmse}}^T$ is given by [15, p. 480]

$$\mathbf{g}_{\text{mmse}}^T = \sigma_s^2\mathbf{c}^{\mathcal{H}}\left(\mathbf{R}_{ww} + \sigma_s^2\mathbf{c}\mathbf{c}^{\mathcal{H}}\right)^{-1} = \frac{\sigma_s^2}{1+\sigma_s^2\mathbf{c}^{\mathcal{H}}\mathbf{R}_{ww}^{-1}\mathbf{c}}\mathbf{c}^{\mathcal{H}}\mathbf{R}_{ww}^{-1} \tag{13}$$

where the matrix inversion lemma has been applied to establish the second equality. Since $\sigma_s^2/\left(1 + \sigma_s^2\mathbf{c}^{\mathcal{H}}\mathbf{R}_{ww}^{-1}\mathbf{c}\right)$ is a constant scalar, the linear MMSE receiver is taken as $\mathbf{g}_{\text{mmse}}^T = \mathbf{c}^{\mathcal{H}}\mathbf{R}_{ww}^{-1}$. In the white noise case, $\mathbf{R}_{ww} = \sigma_w^2\mathbf{I}$, and $\mathbf{g}_{\text{mmse}}^T = \left(1/\sigma_w^2\right)\mathbf{c}^{\mathcal{H}} \propto \mathbf{g}_{\text{mf}}^T$, i.e., the MMSE receiver reduces to the MF, as expected (note that multiplying $\mathbf{g}_{\text{mf}}^T$ by a constant does not affect its performance).

With $\mathbf{g}_{\text{mmse}}^T = \mathbf{c}^{\mathcal{H}}\mathbf{R}_{ww}^{-1}$, the output SNR is obtained as

$$\text{SNR}_{\text{mmse}} := \frac{E\left\{\left|\mathbf{g}_{\text{mmse}}^T\mathbf{c}s\right|^2\right\}}{E\left\{\left|\mathbf{g}_{\text{mmse}}^T\mathbf{w}\right|^2\right\}} = \sigma_s^2\mathbf{c}^{\mathcal{H}}\mathbf{R}_{ww}^{-1}\mathbf{c}. \tag{14}$$

In this section, we developed an unifying framework which describes both MS-SS and DS-SS; we then derived an expression for the SNR at the output of the MF and MMSE receivers. In Section III, we will compare the two modulation schemes in the presence of NBI. The differences are induced by the different equivalent signature vectors $\mathbf{c}$ in (10) and (11), which lead to different output SNR's as given by (12) and (14).

Remark 1: Notice that we adopted a modified implementation for DS-SS. We discarded L chips to remove IBI and enable a simple block by block processing at the receiver. More complex receivers can improve performance of DS-SS by utilizing multiple blocks. Assuming all adjacent symbols are detected perfectly by a genie decoder and their contributions are subtracted from the received data corresponding to the current symbol, the performance of DS-SS is lower-bounded by the benchmark system assuming only one data symbol is transmitted in DS-SS. In such case, we collect $P+L$ samples to form $\mathbf{x}'(i) = [x(iP), x(iP+1), \ldots, x(iP+P+L-1)]^T$. Then $\mathbf{x}'(i)$ can be written as $\mathbf{x}'(i) = \mathbf{C}'_{\text{ds}}\mathbf{h}s(i) + \mathbf{w}'(i)$, where $\mathbf{C}'_{\text{ds}}$ is $(P+L) \times (L+1)$ Toeplitz with first column $\mathbf{c}'_{\text{ds}} := \left[\mathbf{c}_{\text{ds}}^T, \mathbf{0}_{1\times L}\right]^T$ and first row $[c_{\text{ds}}(0), 0, \ldots, 0]$. Comparing this benchmark system to the modified implementation of (11), the only difference is that it uses the equivalent code $\mathbf{c}'_{\text{ds}}$ with energy P, rather than $\bar{\mathbf{c}}_{\text{ds}}$ with energy N. Therefore, this modified implementation differs from the benchmark system by a power deficit of $10\log_{10}(P/N)$ dB, which becomes small when $L \ll N$. The performance of complex receivers for DS-SS can only approximate this benchmark system, and really depends on the chosen receiver type; hence, for simplicity, we compare MC-SS with this modified DS-SS. On the other hand, replacing

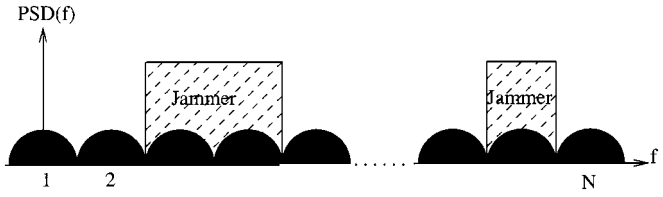

Fig. 2. Signal and interference spectra: a simple example.

$\mathbf{c}$ in (11) by $\mathbf{c} = \mathbf{C}'_{\rm ds}\mathbf{h}$, our theoretical analysis is valid and the resulting closed-form symbol error probability of (47) still provides a lower bound for DS-SS with arbitrary receivers.

III. AWGN Plus Narrow Band Interference

In this section, we focus on the ability of digital MC-SS and DS-SS to suppress narrowband interference. We will assume the channel is nonfading AWGN, i.e., $L = 0$, and $\mathbf{h} = h(0) = 1$. This case was also considered in [14] to compare DS-SS with FD-SS, which is the analog counterpart of the digital MC-SS that we developed in Section II.

Due to the existence of NBI/PBI, the composite noise $\bar{\mathbf{w}}(i)$ in (3) is no longer white. We define its $N \times N$ correlation matrix as: $\mathbf{R}_{\bar{w}\bar{w}} := E\left\{\bar{\mathbf{w}}(i)\bar{\mathbf{w}}^{\mathcal{H}}(i)\right\}$. Since the entries of $\bar{\mathbf{w}}(i)$ are samples from a stationary Gaussian process, we can approximate its correlation matrix by a circulant matrix when the size N is large [2, pp. 73–74]. Therefore, we can approximately diagonalize the correlation matrix by (I)FFT matrices; we assume that the diagonalization is perfect:

As1) $\mathbf{F}_N\mathbf{R}_{\bar{w}\bar{w}}\mathbf{F}_N^{\mathcal{H}} = \mathbf{\Delta}$, *where* $\mathbf{\Delta}$ *is a diagonal matrix with positive diagonal entries* $\delta_{11}, \ldots, \delta_{NN}$.

Because the FFT is asymptotically equivalent to the Karhunen–Loève transform (KLT) [12, p. 461], the entries of the FFT output $\mathbf{F}_N\bar{\mathbf{w}}(i)$ are asymptotically uncorrelated random variables [2]. Therefore, assumption As1) becomes more and more accurate as the FFT size N increases (i.e., the spreading code length increases). See Remark 2 when As1) does not hold exactly.

For illustrative purposes, we construct a simple example, where we assume that the jammer has the same power in every subband where it is present; see Fig. 2 and also [14], [16] for related examples. Thus, the $N \times N$ diagonal matrix $\mathbf{\Delta}$ in As1) has entries

$$\delta_{ii} = \begin{cases} \dfrac{J_0 + N_0}{2}, & \text{if jammer is present in the } i\text{th subband} \\ \dfrac{N_0}{2}, & \text{if jammer is absent in the } i\text{th subband} \end{cases} \tag{15}$$

where $N_0/2$ is the power spectrum density (PSD) of the additive white noise $\eta_c(t)$, and $J_0/2$ is the PSD of the narrowband jammer. Suppose that $\vartheta_c(t)$ occupies ϵB bandwidth ($0 < \epsilon < 1$), which implies that there are ϵN (we assume ϵN to be integer for simplicity) subbands hit by jammers. We can then rewrite $\mathbf{\Delta}$ as

$$\mathbf{\Delta} = \left(\frac{N_0}{2}\right)\mathbf{I}_N + \left(\frac{J_0}{2}\right)\mathbf{I}'_N \tag{16}$$

where $\mathbf{I}'_N$ has ϵN unity entries on the diagonal (if NBI/PBI is present in those subbands), and all other entries are zero.

We now evaluate the SNR and bit error rate (BER) for MC-SS and DS-SS; for simplicity, we assume BPSK modulation in this section. Given SNR, the BER or symbol error rate (SER) expression for other constellations can be similarly found [21].

A. MC-SS

Under As1), we obtain the noise correlation matrix for MC-SS as

$$\mathbf{R}_{ww}^{(\rm mc)} = \mathbf{F}_N\mathbf{R}_{\bar{w}\bar{w}}\mathbf{F}_N^{\mathcal{H}} = \mathbf{\Delta}. \tag{17}$$

With $\mathbf{h} = h(0) = 1$, $\mathbf{c} = \mathbf{D}(\mathbf{c}_{\rm mc})\mathbf{V}\mathbf{h} = \mathbf{c}_{\rm mc}$ in (10), and $\mathbf{R}_{ww}^{(\rm mc)}$ given by (17), we can simplify (12) and (14) for MC-SS as

$$\mathrm{SNR}_{\rm mf}^{(\rm mc)} = \frac{N^2\sigma_s^2}{\mathrm{tr}\{\mathbf{\Delta}\}}, \quad \mathrm{SNR}_{\rm mmse}^{(\rm mc)} = \sigma_s^2\mathrm{tr}\{\mathbf{\Delta}^{-1}\} \tag{18}$$

where $\mathrm{tr}\{\cdot\}$ is the trace operator, and we relied on the fact that the entries of $\mathbf{c}_{\rm mc}$ have unit amplitude to obtain: $\mathrm{tr}\{\mathbf{\Delta}\} = \mathbf{c}_{\rm mc}^{\mathcal{H}}\mathbf{\Delta}\mathbf{c}_{\rm mc}$. Since the arithmetic mean cannot be smaller than the harmonic mean, we have $\mathrm{tr}\{\mathbf{\Delta}^{-1}\} \geq N^2/\mathrm{tr}\{\mathbf{\Delta}\}$, so that $\mathrm{SNR}_{\rm mmse}^{(\rm mc)} \geq \mathrm{SNR}_{\rm mf}^{(\rm mc)}$, as expected (see Appendix I). We infer that the MMSE receiver outperforms the MF receiver, which, of course, is suboptimal in the presence of colored noise.

In the special case of (16), we have $\mathrm{tr}\{\mathbf{\Delta}\} = N(N_0/2 + \epsilon J_0/2)$ and $\mathrm{tr}\{\mathbf{\Delta}^{-1}\} = N[2\epsilon/(J_0+N_0)+2(1-\epsilon)/N_0]$, such that (18) becomes

$$\begin{aligned} \mathrm{SNR}_{\rm mf}^{(\rm mc)} &= \frac{2N\sigma_s^2}{N_0}\frac{1}{1+\epsilon\frac{J_0}{N_0}} \\ \mathrm{SNR}_{\rm mmse}^{(\rm mc)} &= \frac{2N\sigma_s^2}{N_0}\left(\frac{\epsilon}{1+\frac{J_0}{N_0}} + 1 - \epsilon\right). \end{aligned} \tag{19}$$

Define the bit energy $E_b := N\sigma_s^2$, $\beta_{\rm mf}^{(\rm mc)} := 1/(1+\epsilon J_0/N_0)$, and $\beta_{\rm mmse}^{(\rm mc)} = \epsilon/(1+J_0/N_0)+1-\epsilon$. Based on (19), the corresponding closed-form BER expressions for BPSK can be found as [21, p. 258]:

$$P_{b,\rm mf}^{(\rm mc)} = \mathcal{Q}\left(\sqrt{\frac{2E_b}{N_0}\beta_{\rm mf}^{(\rm mc)}}\right) \quad P_{b,\rm mmse}^{(\rm mc)} = \mathcal{Q}\left(\sqrt{\frac{2E_b}{N_0}\beta_{\rm mmse}^{(\rm mc)}}\right). \tag{20}$$

where $\mathcal{Q}(\cdot)$ denotes the $\mathcal{Q}$-function. Parameters $\beta_{\rm mf}^{(\rm mc)}$ and $\beta_{\rm mmse}^{(\rm mc)}$ are both less than unity and indicate the SNR loss for MC-SS relative to transmission over an AWGN channel with $\mathrm{SNR} = 2E_b/N_0$. In order to achieve the same error probability as in the unjammed AWGN case, bit energy E_b must be increased by a factor of $1/\beta_{\rm mf}^{(\rm mc)}$ or $1/\beta_{\rm mmse}^{(\rm mc)}$.

As J_0/N_0 increases, both $\beta_{\rm mf}^{(\rm mc)}$ and $\beta_{\rm mmse}^{(\rm mc)}$ decrease and consequently the BER performance degrades as confirmed by (20). However, one can notice that the SNR degradation is unbounded for the MF receiver, but is upper bounded for the MMSE receiver even when $J_0/N_0 \to \infty$, since the power degradation $1/\beta_{\rm mmse}^{(\rm mc)} \leq 1/(1-\epsilon)$. To compare these two different receivers more clearly, we define the SNR gain of MMSE over MF receiver as:

$$\mathcal{G} := \frac{\beta_{\rm mmse}^{(\rm mc)}}{\beta_{\rm mf}^{(\rm mc)}} = 1 + \epsilon(1-\epsilon)\frac{\left(\frac{J_0}{N_0}\right)^2}{1+\frac{J_0}{N_0}}. \tag{21}$$

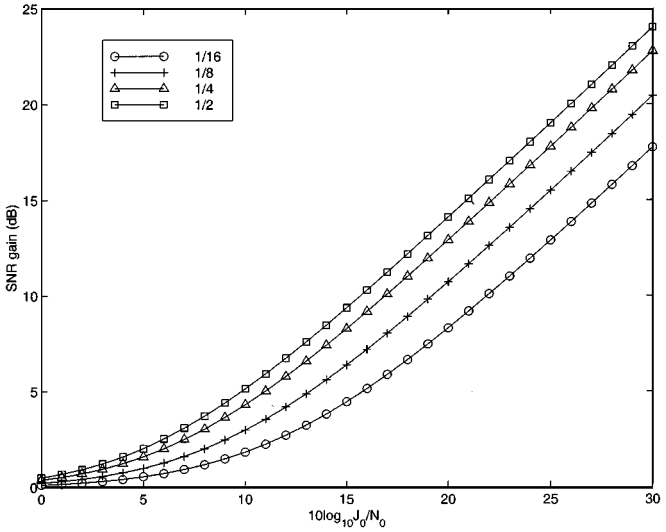

Fig. 3. SNR gain of MMSE over MF receiver as a function of interference power to AWGN variance, with curves parameterized by ϵ, the fractional bandwidth of the interference.

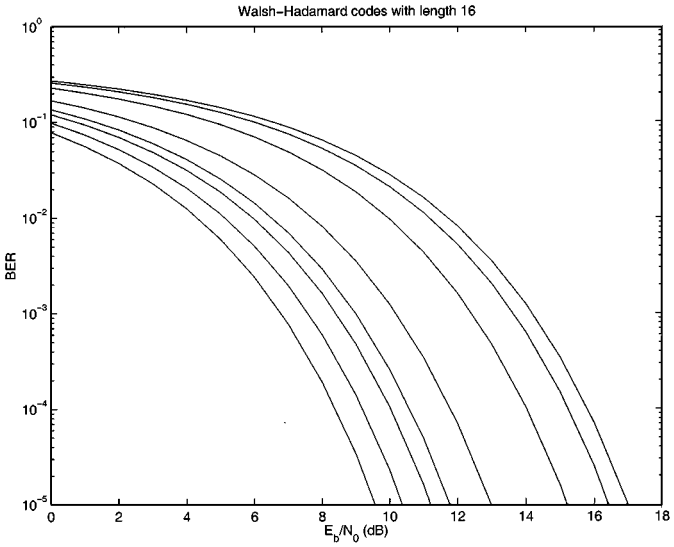

Fig. 4. BER for DS-SS with different W–H codes of length $P = 16$. MF receiver is used. The jammer has $\epsilon = 3/16$ and $10\log_{10}(J_0/N_0) = 10$ dB. This figure is to show the performance difference with different W–H codes.

From (21), we find that $\beta_{\rm mmse}^{(\rm mc)} \geq \beta_{\rm mf}^{(\rm mc)}$, with equality at $\epsilon = 0$ (no NBI) or $\epsilon = 1$ (NBI occupies the full band); both of these cases correspond to white noise. In Fig. 3, we plot the SNR gain in (21) versus power density ratio J_0/N_0, for different values of the NBI parameter $\epsilon = [1/16, 1/8, 1/4, 1/2]$. Even for a moderate power NBI, say with $\epsilon = 1/16$, and $J_0/N_0 = 15$ dB, the gain is 5 dB, and increases with ϵ and J_0/N_0. In the presence of colored noise, the linear MMSE receiver significantly outperforms the MF receiver, especially as the power spectrum density of NBI and the jammed bandwidth percentage increase. For a fixed J_0/N_0, the SNR gain $\mathcal{G}$ peaks at $\epsilon = 1/2$ which can be inferred from (21). Given a fixed average jamming power $J = \epsilon W_x J_0$ (W_x denotes the system bandwidth), it has been shown in [14] that the worst jammer for the MMSE receiver spreads its power evenly over the entire signal bandwidth, i.e., $\epsilon = 1$; in this case, the MMSE receiver reduces to the conventional MF receiver and thus the SNR gain becomes $\mathcal{G} = 1$.

In this subsection, we showed that the MMSE receiver (which has knowledge of which subbands are jammed, and the jammer power to AWGN ratio) outperforms the MF receiver; the SNR gain of the MMSE receiver with respect to the MF receiver, $\mathcal{G}$ of (21), increases as the jammer power or the bandwidth occupied by the jammer increases. Further, a smart adversary spreads its power evenly[2], so that the MF (equivalent to MMSE now) is optimal. The SNR/BER performance is independent of the spreading code.

B. DS-SS

For DS-SS, we have $P = N$, $\mathbf{c} = \mathbf{C}\mathbf{h} = \bar{\mathbf{c}}_{\rm ds} = \mathbf{c}_{\rm ds}$ in (11), and $\mathbf{R}_{ww}^{(\rm ds)} = \mathbf{R}_{\bar{w}\bar{w}} = \mathbf{F}_N^{\mathcal{H}}\mathbf{\Delta}\mathbf{F}_N$ as per As1); the SNR in (12) and (14) can be simplified as

$$\begin{aligned}\mathrm{SNR}_{\rm mf}^{(\rm ds)} &= \frac{N^2\sigma_s^2}{\mathbf{c}_{\rm ds}^{\mathcal{H}}\mathbf{F}_N^{\mathcal{H}}\mathbf{\Delta}\mathbf{F}_N\mathbf{c}_{\rm ds}} \\ \mathrm{SNR}_{\rm mmse}^{(\rm ds)} &= \sigma_s^2\mathbf{c}_{\rm ds}^{\mathcal{H}}\mathbf{F}_N^{\mathcal{H}}\mathbf{\Delta}^{-1}\mathbf{F}_N\mathbf{c}_{\rm ds}. \end{aligned} \quad (22)$$

[2]A smart jammer could hop thus making it difficult to estimate the jammer power; we do not consider this scenario in this paper.

We see from (22) that the SNR's for DS-SS are *code dependent*, in contrast with the case for MC-SS in (18). Thus, the BER performance will be different for differently chosen spreading codes $\mathbf{c}_{\rm ds}$. We illustrate this in Fig. 4 where the BER performance of the MF receiver for DS-SS, $P_{b,\rm mf}^{(\rm ds)} = \mathcal{Q}\left(\left[\mathrm{SNR}_{\rm mf}^{(\rm ds)}\right]^{1/2}\right)$, is depicted for different Walsh–Hadamard (W–H) codes of length $P = 16$ in the presence of a jammer with $\epsilon = 3/16$ and $10\log_{10}(J_0/N_0) = 10$ dB. Intuitively speaking, the spectrum of any particular code vector, $\mathbf{c}_{\rm ds}$, is generally not flat. When the jammer hits the subband where the signal power is strong, the BER degradation becomes more pronounced, which leads to considerably different performance for different codes as depicted in Fig. 4.

To avoid the code dependence and improve the performance of DS-SS, two approaches can be taken. The first is to design a spreading code with unit amplitude in both time and frequency, i.e., with the entries of $\mathbf{F}_N\mathbf{c}_{\rm ds}$ having unit amplitude. With such codes, we obtain the same result as in (18), which implies that DS-SS can have the same performance as MC-SS. Such a code exists, as explained below.

Consider the periodic auto correlation function (PACF) of an $N \times 1$ code $\mathbf{a} := [a(0), a(1), \ldots, a(N-1)]^T$ defined as: $\Psi_{\mathbf{a}}(k) = \sum_n a^*(n)a(n+k \bmod N)$, $k = 0, \ldots, N-1$. Let $\delta(k)$ denotes Kronecker's delta, and assume that the following condition holds true: $\Psi_{\mathbf{a}}(k) = N\delta(k)$, i.e., $\Psi_{\mathbf{a}}(k)$ has a single peak at $k = 0$, the code is said to have perfect PACF [6], [9], [13]. To design a code with flat spectrum, it is necessary and sufficient to design a code with perfect PACF, as asserted by the following lemma.

Lemma 1: For any $N \times 1$ code vector $\mathbf{a}$, the following two conditions are equivalent:

1) code $\mathbf{a}$ has perfect PACF, i.e., $\Psi_{\mathbf{a}}(k) = N\delta(k)$;
2) code has flat spectrum, i.e., the entries of $\mathbf{F}_N\mathbf{a}$ are of unit amplitude.

Proof: Define the $N \times N$ cyclic shift matrix $\mathbf{Z}$ with output $\mathbf{Z}\mathbf{a} = [a(N-1), a(0), \ldots, a(N-2)]^T$, when operating on the

vector $\mathbf{a}$. Consider now the circulant matrix $\mathbf{A} = \text{circ}(\mathbf{a}) := [\mathbf{a}, \mathbf{Z}\mathbf{a}, \ldots, \mathbf{Z}^{N-1}\mathbf{a}]$. Since $\mathbf{A}$ is circulant, it is diagonalizable by (I)FFT matrices (see e.g., [26] for details):

$$\mathbf{F}_N \mathbf{A} \mathbf{F}_N^{\mathcal{H}} = \mathbf{D}\left(\sqrt{N}\mathbf{F}_N \mathbf{a}\right) \text{ and } \mathbf{A} = \mathbf{F}_N^{\mathcal{H}} \mathbf{D}\left(\sqrt{N}\mathbf{F}_N \mathbf{a}\right)\mathbf{F}. \tag{23}$$

Condition 1 requires that $\mathbf{A}^{\mathcal{H}}\mathbf{A} = N\mathbf{I}_N$, while condition 2 amounts to $\mathbf{D}^{\mathcal{H}}(\mathbf{F}_N\mathbf{a})\mathbf{D}(\mathbf{F}_N\mathbf{a}) = \mathbf{I}_N$. Based on (23), it is clear that these two conditions are equivalent:

$$\mathbf{A}^{\mathcal{H}}\mathbf{A} = N\mathbf{I}_N \Leftrightarrow \mathbf{D}^{\mathcal{H}}(\mathbf{F}_N\mathbf{a})\mathbf{D}(\mathbf{F}_N\mathbf{a}) = \mathbf{I}_N. \tag{24}$$

In [22], the Frank and Zadoff PACF sequence of [9] was shown to have flat spectrum. Here, we have provided a general proof and established that conditions 1 and 2 are equivalent. ■

Therefore, if DS-SS employs any code with perfect PACF, e.g., the constant amplitude zero autocorrelation (CAZAC) sequences of [6], [9], [13] (see also [18], [22] and references therein), it has the same performance as MC-SS. Although perfect autocorrelation property is achieved for each CAZAC sequence, the cross-correlations between different CAZAC sequences might be large. For this reason, the CAZAC sequences have gained their popularity in applications of synchronization and channel estimation [13], [18], [22], but have limited usage in spread spectrum systems that are designed to allow for multiple access. Next, we focus on commonly used spreading codes that unfortunately do not possess perfect PACF.

To avoid the dependence of system performance on codes not having perfect PACF, we may adopt either code hopping (a scheme where each user in a short code system switches among a predetermined set of code sequences [20]), or long code spreading, where the code period is much larger than the symbol period [20]. Let us suppose that there are N_c codes in a code hopping system with codes $\{\mathbf{c}_{\text{ds},n}\}_{n=1}^{N_c}$. Let $\text{SNR}_{\text{mf},n}^{(\text{ds})}$ denote the output SNR resulting from the nth code, obtained by substituting $\mathbf{c}_{\text{ds}}$ in (22) with $\mathbf{c}_{\text{ds},n}$. Assuming that each code is picked with equal probability, the *averaged* SNR and BER (over the code set) for the MF receiver are then given by

$$\begin{aligned} \text{SNR}_{\text{mf}}^{(\text{ds})} &= \frac{1}{N_c}\sum_{n=1}^{N_c} \text{SNR}_{\text{mf},n}^{(\text{ds})} \\ P_{b,\text{mf}}^{(\text{ds})} &= \frac{1}{N_c}\sum_{n=1}^{N_c} \mathcal{Q}\left(\sqrt{\text{SNR}_{\text{mf},n}^{(\text{ds})}}\right). \end{aligned} \tag{25}$$

For long code spreading, we assume that the code period is sufficiently long so that the chips can be thought of as being uncorrelated, i.e., $E\left\{\mathbf{c}_{\text{ds}}\mathbf{c}_{\text{ds}}^{\mathcal{H}}\right\} = \mathbf{I}_N$. Then, we have

$$\begin{aligned} E_{\mathbf{c}_{\text{ds}}}\left\{\mathbf{c}_{\text{ds}}^{\mathcal{H}}\mathbf{F}_N^{\mathcal{H}}\mathbf{\Delta}\mathbf{F}_N\mathbf{c}_{\text{ds}}\right\} &= \text{tr}\left\{E_{\mathbf{c}_{\text{ds}}}\left\{\mathbf{c}_{\text{ds}}\mathbf{c}_{\text{ds}}^{\mathcal{H}}\mathbf{F}_N^{\mathcal{H}}\mathbf{\Delta}\mathbf{F}_N\right\}\right\} \\ &= \text{tr}\{\mathbf{\Delta}\} \end{aligned}$$

which results in an average SNR

$$E_{\mathbf{c}_{\text{ds}}}\left\{\text{SNR}_{\text{mf}}^{(\text{ds})}\right\} = \frac{N^2\sigma_s^2}{\text{tr}\{\mathbf{\Delta}\}} = \text{SNR}_{\text{mf}}^{(\text{mc})}. \tag{26}$$

Similarly, we can obtain $E_{\mathbf{c}_{\text{ds}}}\left\{\mathbf{c}_{\text{ds}}^{\mathcal{H}}\mathbf{F}_N^{\mathcal{H}}\mathbf{\Delta}^{-1}\mathbf{F}_N\mathbf{c}_{\text{ds}}\right\} = \text{tr}\{\mathbf{\Delta}^{-1}\}$ and

$$E_{\mathbf{c}_{\text{ds}}}\left\{\text{SNR}_{\text{mmse}}^{(\text{ds})}\right\} = \sigma_s^2\text{tr}\left\{\mathbf{\Delta}^{-1}\right\} = \text{SNR}_{\text{mmse}}^{(\text{mc})}. \tag{27}$$

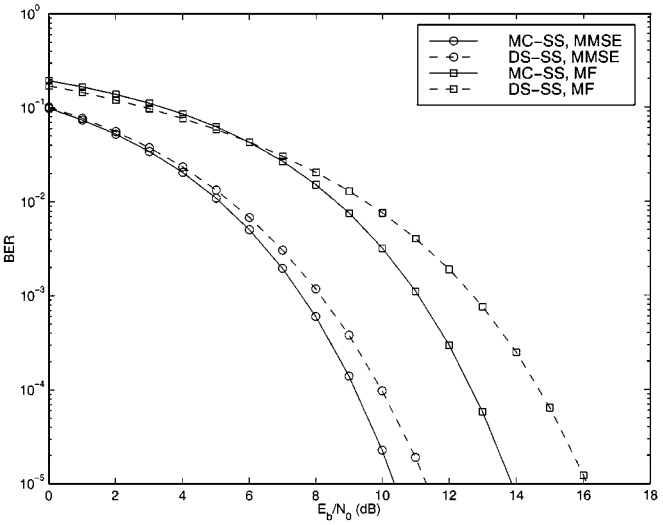

Fig. 5. MC-SS versus DS-SS, code hopping.

Although the average SNR's for long-code DS-SS coincides with those for MC-SS with symbol-periodic codes, the average BERs

$$\begin{aligned} P_{b,\text{mf}}^{(\text{ds})} &= E_{\mathbf{c}_{\text{ds}}}\left\{\mathcal{Q}\left(\sqrt{\text{SNR}_{\text{mf}}^{(\text{ds})}}\right)\right\} \\ P_{b,\text{mmse}}^{(\text{ds})} &= E_{\mathbf{c}_{\text{ds}}}\left\{\mathcal{Q}\left(\sqrt{\text{SNR}_{\text{mmse}}^{(\text{ds})}}\right)\right\} \end{aligned} \tag{28}$$

may differ, because in general

$$E_{\mathbf{c}_{\text{ds}}}\left\{\mathcal{Q}\left(\sqrt{\text{SNR}_{\text{mf}}^{(\text{ds})}}\right)\right\} \neq \mathcal{Q}\left(\sqrt{E_{\mathbf{c}_{\text{ds}}}\left\{\left(\text{SNR}_{\text{mf}}^{(\text{ds})}\right)\right\}}\right).$$

The latter implies that $P_{b,\text{mf}}^{(\text{ds})} \neq P_{b,\text{mf}}^{(\text{mc})}$, and similarly $P_{b,\text{mmse}}^{(\text{ds})} \neq P_{b,\text{mf}}^{(\text{mmse})}$. Note that the SNR's in (18) for MC-SS do not change with different $\mathbf{c}_{\text{mc}}$'s while the SNR's for DS-SS fluctuate around their means given by (26) and (27), if codes not having perfect PACF are used for DS-SS. Since $\mathcal{Q}(\sqrt{x})$ is convex in x, we obtain

$$P_{b,\text{mf}}^{(\text{ds})} \geq P_{b,\text{mf}}^{(\text{mc})}, \quad P_{b,\text{mmse}}^{(\text{ds})} \geq P_{b,\text{mmse}}^{(\text{mc})} \tag{29}$$

by applying the Jensen's inequality $E\{f(x)\} \geq f(E\{x\})$ for a convex function $f(x)$ [7, p. 25]. Equation (29) also verifies the intuition that the average BER is dominated by worst cases. However, the difference becomes small when the code period is sufficiently long. In Fig. 5, we plot the average BER [cf. (25)] of a code hopping system with codes selected from the set of W–H codes of length 16. MC-SS has a 2 dB advantage over DS-SS at BER of 10^{-5} if MF is used. In Fig. 6, the BER of a long code spreading DS-SS system [cf. (28)] is depicted with period 1000 times the symbol period of $P = 16$ chips. In both cases, the jammer is the same as in Fig. 4. Comparing Fig. 5 with Fig. 6, we see that as the randomness of the code increases (code period increases), DS-SS performance approaches that of MC-SS.

Assuming long code spreading in DS-SS, the MF receiver and the average SNR expression of (26) were also derived in [14]. By assuming tacitly

$$E_{\mathbf{c}_{\text{ds}}}\left\{\mathcal{Q}\left(\left[\text{SNR}_{\text{mf}}^{(\text{ds})}\right]^{1/2}\right)\right\} = \mathcal{Q}\left(\left[E_{\mathbf{c}_{\text{ds}}}\left\{\text{SNR}_{\text{mf}}^{(\text{ds})}\right\}\right]^{1/2}\right)$$

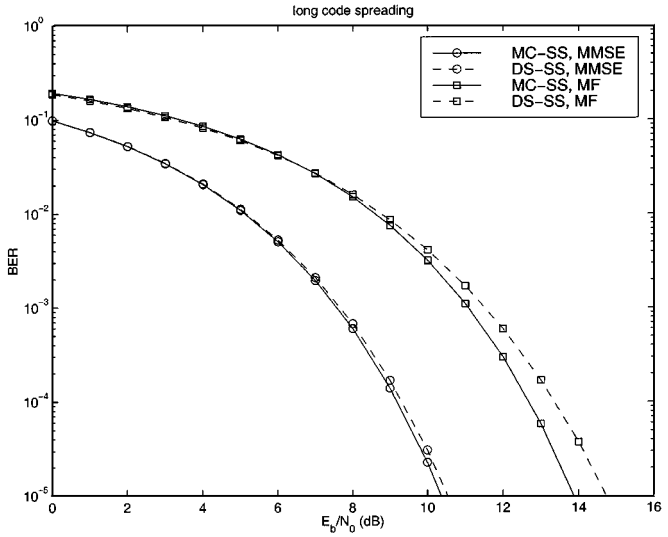

Fig. 6. MC-SS versus DS-SS, long codes.

and thus $P_{b,\mathrm{mf}}^{(\mathrm{ds})} = P_{b,\mathrm{mf}}^{(\mathrm{mc})}$, it was asserted in [14] that

$$P_{b,\mathrm{mf}}^{(\mathrm{ds})} \geq P_{b,\mathrm{mmse}}^{(\mathrm{mc})} \tag{30}$$

with the SNR gain of MC-SS over DS-SS equal to that given in (21).

The motivation behind adopting the MMSE receiver for FD-SS (MC-SS) and the MF receiver for DS-SS in [14] is implementation complexity. It turns out that the MMSE receiver is easy to build for analog MC-SS while it is difficult for DS-SS [14]. In contrast, with our digital transceivers, implementing MF or MMSE receivers for both MC-SS and DS-SS entails comparable complexity. The MMSE receiver can be constructed after estimating the interference color by training or via blind adaptive algorithms. With the same kind of receivers for both systems, the DS-SS can have the same performance as MC-SS, unlike the analog implementations in [14] where MC-SS and DS-SS employ different receivers, if a CAZAC sequence is employed for DS-SS. For widely used spreading sequences with imperfect PACF, although the conclusion that MC-SS is more robust to NBI than DS-SS has been reached here, we see that the differences are much less pronounced.

Remark 2: If As1) does not hold exactly for the MC-SS, we can express $\mathbf{F}_N\mathbf{R}_{\bar{w}\bar{w}}\mathbf{F}_N^{\mathcal{H}} = \mathbf{\Delta} + \mathbf{E}$, where $\mathbf{E}$ is a perturbation matrix having entries with small amplitudes. For MC-SS, $\mathbf{c}^{\mathcal{H}}\mathbf{R}_{ww}\mathbf{c} = \mathbf{c}_{\mathrm{mc}}^{\mathcal{H}}\mathbf{F}_N\mathbf{R}_{\bar{w}\bar{w}}\mathbf{F}_N^{\mathcal{H}}\mathbf{c}_{\mathrm{mc}} = \mathrm{tr}\{\mathbf{\Delta}\} + \mathbf{c}_{\mathrm{mc}}^{\mathcal{H}}\mathbf{E}\mathbf{c}_{\mathrm{mc}}$. Now, the SNR's in (12) and (14) for MC-SS also depend on the choice of the spreading code (in contrast with the case where $\mathbf{E} = \mathbf{0}$, leading to (18)). If we use code hopping or long code spreading, we can obtain the average SNR's following the same approach as that for the DS-SS

$$E_{\mathbf{c}_{\mathrm{mc}}}\left\{\mathrm{SNR}_{\mathrm{mf}}^{(\mathrm{mc})}\right\} = \frac{N^2\sigma_s^2}{\mathrm{tr}\left\{\mathbf{R}_{\bar{w}\bar{w}}\right\}} = E_{\mathbf{c}_{\mathrm{ds}}}\left\{\mathrm{SNR}_{\mathrm{mf}}^{(\mathrm{ds})}\right\} \tag{31}$$

$$E_{\mathbf{c}_{\mathrm{mc}}}\left\{\mathrm{SNR}_{\mathrm{mmse}}^{(\mathrm{mc})}\right\} = \sigma_s^2\mathrm{tr}\left\{\mathbf{R}_{\bar{w}\bar{w}}^{-1}\right\} = E_{\mathbf{c}_{\mathrm{ds}}}\left\{\mathrm{SNR}_{\mathrm{mmse}}^{(\mathrm{ds})}\right\}. \tag{32}$$

Although the average SNR is the same, we expect that the average BER is somewhat lower for MC-SS than for DS-SS equipped with codes having imperfect PACF, because the SNR for MC-SS has smaller fluctuations due to the fact that the perturbation matrix $\mathbf{E}$ is negligible, i.e., As1) is basically satisfied.

In this subsection, we showed that the performance of DS-SS is code dependent; in order to eliminate this code dependence, we either need to construct spreading codes with perfect PACF, or hop among codes, or use long codes. If codes with perfect PACF are used, the performance of DS-SS coincides with that of MC-SS. For widely used spreading codes with imperfect PACF, MC-SS outperforms DS-SS in general, while the performance difference decreases as the period of the (long) code increases. The performance of MC-SS also becomes code dependent if the noise is nonstationary; code hopping is useful in this case. Recall that in this section, we assumed that the degradation is only due to AWGN and NBI/PBI.

IV. Random Multipath Fading Channels

In this section, we focus on multipath fading channels and assume that NBI is absent and the additive noise is white, i.e., $\mathbf{R}_{\bar{w}\bar{w}} = \sigma_w^2\mathbf{I}_N$. In this case, the MMSE receiver $\mathbf{g}_{\mathrm{mmse}}^T = \left(1/\sigma_w^2\right)\mathbf{c}^{\mathcal{H}}$ and the MF receiver $\mathbf{g}_{\mathrm{mf}}^T = \mathbf{c}^{\mathcal{H}}$ achieve the same performance, and the output SNR becomes $\mathrm{SNR} = \mathbf{c}^{\mathcal{H}}\mathbf{c}\sigma_s^2/\sigma_w^2$, where $\mathbf{c}$ is defined in (10) for MC-SS and in (11) for DS-SS.

Recall that $\mathbf{c} = \mathbf{D}(\mathbf{c}_{\mathrm{mc}})\mathbf{V}\mathbf{h}$ for MC-SS and $\mathbf{c} = \bar{\mathbf{C}}_{\mathrm{ds}}\mathbf{h}$ for DS-SS. For spreading codes $\mathbf{c}_{\mathrm{mc}}$ and $\mathbf{c}_{\mathrm{ds}}$ with unit amplitude entries, the corresponding SNR's for a given channel $\mathbf{h}$ are

$$\mathrm{SNR}^{(\mathrm{mc})} = \frac{\mathbf{h}^{\mathcal{H}}\mathbf{V}^{\mathcal{H}}\mathbf{D}^{\mathcal{H}}(\mathbf{c}_{\mathrm{mc}})\mathbf{D}(\mathbf{c}_{\mathrm{mc}})\mathbf{V}\mathbf{h}\sigma_s^2}{\sigma_w^2} = \frac{N\mathbf{h}^{\mathcal{H}}\mathbf{h}\sigma_s^2}{\sigma_w^2} \tag{33}$$

$$\mathrm{SNR}^{(\mathrm{ds})} = \frac{\mathbf{h}^{\mathcal{H}}\bar{\mathbf{C}}_{\mathrm{ds}}^{\mathcal{H}}\bar{\mathbf{C}}_{\mathrm{ds}}\mathbf{h}\sigma_s^2}{\sigma_w^2}. \tag{34}$$

Equation (33) clearly shows that the SNR, and thus the BER, in MC-SS do not depend on the code choices while they do in DS-SS. In [16] it is assumed that the self-interference due to multipath is *negligible*, i.e., the shifts of the spreading code are nearly orthogonal to itself so that $\bar{\mathbf{C}}_{\mathrm{ds}}^{\mathcal{H}}\bar{\mathbf{C}}_{\mathrm{ds}} = N\mathbf{I}_{L+1}$. Under this assumption, we have that $\mathrm{SNR}^{(\mathrm{mc})} = \mathrm{SNR}^{(\mathrm{ds})}$, which indicates that MC-SS and DS-SS exhibit the same ability in resisting multipath effects, which agrees with the results in [16]. In general, the Toeplitz matrix $\bar{\mathbf{C}}_{\mathrm{ds}}$ does not have orthogonal columns. The columns of $\bar{\mathbf{C}}_{\mathrm{ds}}$ can be approximately orthogonal (thus self-interference is negligible) only when the code length P is sufficiently large relative to the channel order L and the code is well constructed. Unlike [16], where focus is placed on multiuser interference and narrowband interference but the multipath-induced self-interference is ignored, here, we explicitly consider this self-interference effect and compare the multipath resistance of DS-SS with that of MC-SS. We study two scenarios: one with $\bar{\mathbf{C}}_{\mathrm{ds}}^{\mathcal{H}}\bar{\mathbf{C}}_{\mathrm{ds}} = N\mathbf{I}_{L+1}$, and the other with $\bar{\mathbf{C}}_{\mathrm{ds}}^{\mathcal{H}}\bar{\mathbf{C}}_{\mathrm{ds}} \neq N\mathbf{I}_{L+1}$.

With carefully constructed codes satisfying $\bar{\mathbf{C}}_{\mathrm{ds}}^{\mathcal{H}}\bar{\mathbf{C}}_{\mathrm{ds}} = N\mathbf{I}_{L+1}$, the self interference in DS-SS is eliminated deterministically. Thus DS-SS achieves the same performance as MC-SS. Such codes exist. The following is one way to construct the $P \times 1$ vector $\mathbf{c}_{\mathrm{ds}}$. We start from the $N \times 1$ vector $\bar{\mathbf{c}}_{\mathrm{ds}}$ and form $\mathbf{c}_{\mathrm{ds}} = \mathbf{T}_{\mathrm{cp}}\bar{\mathbf{c}}_{\mathrm{ds}}$. The latter amounts to a cyclic

prefixed transmission in DS-SS; the difference with MC-SS is that the spreading code here is not processed by IFFT at the transmitter. It can then be verified that each column of $\bar{\mathbf{C}}_{\rm ds}$ is a cyclic shift of $\bar{\mathbf{c}}_{\rm ds}$, and $\bar{\mathbf{C}}_{\rm ds} = \left[\bar{\mathbf{c}}_{\rm ds}, \mathbf{Z}\bar{\mathbf{c}}_{\rm ds}, \ldots, \mathbf{Z}^L\bar{\mathbf{c}}_{\rm ds}\right]$ is the first $L+1$ columns of the $N \times N$ circulant matrix constructed as $\tilde{\mathbf{C}}_{\rm ds} := {\rm circ}(\bar{\mathbf{c}}_{\rm ds}) = \left[\bar{\mathbf{c}}_{\rm ds}, \mathbf{Z}\bar{\mathbf{c}}_{\rm ds}, \ldots, \mathbf{Z}^{N-1}\bar{\mathbf{c}}_{\rm ds}\right]$. We reiterate that for codes with perfect PACF, such as those in [6], [9], [13], [18], we have $\tilde{\mathbf{C}}_{\rm ds}^{\mathcal{H}}\tilde{\mathbf{C}}_{\rm ds} = N\mathbf{I}_N$, and thus $\bar{\mathbf{C}}_{\rm ds}^{\mathcal{H}}\bar{\mathbf{C}}_{\rm ds} = N\mathbf{I}_{L+1}$. Other classes of codes are also possible. To guarantee $\bar{\mathbf{C}}_{\rm ds}^{\mathcal{H}}\bar{\mathbf{C}}_{\rm ds} = N\mathbf{I}_{L+1}$, it is not necessary to use codes with perfect PACF. It is evident that we only need $\Psi_{\bar{\mathbf{c}}_{\rm ds}}(k) = 0$ for $k = 1, 2, \ldots, L$. The general class of spreading sequences with zero correlation zone (ZCZ), i.e., $\Psi_{\bar{\mathbf{c}}_{\rm ds}}(k) = 0$, $|k| \leq L_{\rm ZCZ}$ and $k \neq 0$, are investigated in e.g., [4], [8], where $L_{\rm ZCZ}$ denotes the zone length. If the codes with $L_{\rm ZCZ} \geq L$ are applied in DS-SS, then $\bar{\mathbf{C}}_{\rm ds}^{\mathcal{H}}\bar{\mathbf{C}}_{\rm ds} = N\mathbf{I}_{L+1}$ is satisfied; hence, DS-SS can achieve the same performance as MC-SS.

For widely used codes with $\bar{\mathbf{C}}_{\rm ds}^{\mathcal{H}}\bar{\mathbf{C}}_{\rm ds} \neq N\mathbf{I}_{L+1}$, we next show that the performance of DS-SS degrades relative to that of MC-SS.

For random channels $\mathbf{h}$, with zero mean and covariance matrix $\mathbf{R}_{hh} := E\{\mathbf{h}\mathbf{h}^{\mathcal{H}}\}$, the BER for BPSK can be expressed in terms of the output SNR as

$$P_b = E_{\mathbf{h}}\left\{\mathcal{Q}\left(\sqrt{\rm SNR}\right)\right\}. \tag{35}$$

It is computationally intensive to evaluate (35) by averaging over the statistics of the fading amplitude random variables directly [25], since it entails calculation of $(L+1)$-dimensional infinite integrals. However, by using an alternative representation of $\mathcal{Q}(\cdot)$, a closed-form symbol error rate (SER) expression for a diversity system with multiple flat-faded channels (its system input–output relationship can be described by (38) in our notation) and maximum ratio combining (MRC) at the receiver has been obtained in [25]. Establishing $\mathbf{g}_{\rm mmse}^T$ as an equivalent MRC combiner and using the result of [25], we will first derive a general SER expression for MC-SS and DS-SS, and then compare their capabilities in resisting multipath. The channel estimates at the receiver are assumed to be error-free.

We first diagonalize $\mathbf{R}_{hh}$ using its spectral decomposition

$$\mathbf{R}_{hh} = \mathbf{U}_h\mathbf{D}_h\mathbf{U}_h^{\mathcal{H}}, \quad \mathbf{D}_h = {\rm diag}(\lambda_{11}, \ldots, \lambda_{LL}) \tag{36}$$

where $\mathbf{U}_h$ is unitary and $\lambda_{ii} \geq 0$ is the ith eigenvalue of $\mathbf{R}_{hh}$.

Similarly, we decompose the signature code covariance matrix $\mathbf{R}_{cc} := E\{\mathbf{c}\mathbf{c}^{\mathcal{H}}\}$ as:

$$\mathbf{R}_{cc} = E\{\mathbf{C}\mathbf{h}\mathbf{h}^{\mathcal{H}}\mathbf{C}^{\mathcal{H}}\} = \mathbf{C}\mathbf{R}_{hh}\mathbf{C}^{\mathcal{H}} = \mathbf{U}_c\mathbf{D}_c\mathbf{U}_c^{\mathcal{H}} \tag{37}$$

where $\mathbf{U}_c$ is a $N \times (L+1)$ matrix with orthonormal columns and $\mathbf{D}_c$ is a diagonal matrix with entries $\bar{\lambda}_{ii}, i \in [1, L+1]$. The matrix $\mathbf{R}_{cc}$ has only $L+1$ nonzero eigenvalues because $\mathbf{R}_{hh}$ is of size $(L+1) \times (L+1)$. When $\mathbf{R}_{hh}$ is diagonal and $\mathbf{C}$ has orthonormal columns, we have $\bar{\lambda}_{ii} = \lambda_{ii}, \ \forall\, i \in [1, L+1]$.

Pre-multiplying $\mathbf{y}(i)$ in (9) with $\mathbf{U}_c^{\mathcal{H}}$ yields

$$\begin{aligned}\mathbf{y}'(i) :=& \mathbf{U}_c^{\mathcal{H}}\mathbf{y}(i) = \mathbf{U}_c^{\mathcal{H}}\mathbf{C}\mathbf{h}s(i) + \mathbf{U}_c^{\mathcal{H}}\mathbf{w}(i)\\ :=& \mathbf{h}'s(i) + \mathbf{w}'(i)\end{aligned} \tag{38}$$

where $\mathbf{h}' := \mathbf{U}_c^{\mathcal{H}}\mathbf{C}\mathbf{h}$ and $\mathbf{w}'(i) := \mathbf{U}_c^{\mathcal{H}}\mathbf{w}(i)$ denote, respectively, equivalent channel and noise vectors. Because $\mathbf{R}_{h'h'} = \mathbf{U}_c^{\mathcal{H}}\mathbf{R}_{cc}\mathbf{U}_c = \mathbf{D}_c$, the entries of $\mathbf{h}'$ are uncorrelated, while $\mathbf{w}'(i)$ is still white since $\mathbf{R}_{w'w'} = \sigma_w^2\mathbf{I}_{L+1}$. The MRC based symbol estimate $\hat{s}(i) = (\mathbf{h}')^{\mathcal{H}}\mathbf{y}'(i)$ equals the output of the MMSE or the MF receiver in this white noise case. As a result, a closed form SER expression for MPSK (M constellation points) signals can be obtained by direct substitution from [25, eq. (44)]:

$$P_s(E) = \frac{1}{\pi}\int_0^{(M-1)\pi/M}\prod_{i=1}^{L} I_i\left(\frac{\bar{\lambda}_{ii}\sigma_s^2}{\sigma_w^2}, \gamma_{\rm PSK}, \theta\right)d\theta \tag{39}$$

where $\gamma_{\rm PSK} := \sin^2(\pi/M)$, and $I_i(x, \gamma_{\rm PSK}, \theta)$ is the moment of the probability density function of h_i' evaluated at $-\gamma_{\rm PSK}/\sin^2(\theta)$ (see [25, eq. (24)]). For example, if h_i' is Rayleigh distributed, we have

$$I_i(x, \gamma_{\rm PSK}, \theta) = \left[1 + \frac{\gamma_{\rm PSK}x}{\sin^2(\theta)}\right]^{-1}. \tag{40}$$

The moment $I_i(x, \gamma_{\rm PSK}, \theta)$ for other distributions such as Ricean, Nakagami, and the resulting SER for different constellations (e.g., QAM) can be found in [25]. Note that because $\mathbf{h}'$ is obtained from $\mathbf{h}$ by linear transformations, the moment $I_i(x, \gamma_{\rm PSK}, \theta)$ for h_i' may not be easily tractable for arbitrary distributed $\mathbf{h}$. However, when $\mathbf{h}$ is Gaussian distributed or $\mathbf{h}$ has uncorrelated taps with known distribution listed in [25] and $\mathbf{C}$ has orthogonal columns (e.g., MC-SS), in which case $\mathbf{h}'$ is proportional to $\mathbf{h}$, (39) provides a closed-form expression that can be easily evaluated.

To establish the optimality of MC-SS, let us consider the generic model of [11]

$$\tilde{\mathbf{y}}(i) = \tilde{\mathbf{C}}\mathbf{h}s(i) + \tilde{\mathbf{w}}(i) \tag{41}$$

where $\tilde{\mathbf{w}}(i)$ is white and $\tilde{\mathbf{C}}$ is an arbitrary $N \times (L+1)$ matrix obeying the power constraint: ${\rm tr}\{\tilde{\mathbf{C}}^{\mathcal{H}}\tilde{\mathbf{C}}\} = \mathcal{P}_0$, prescribed by the transmit-power budget.

Starting with the generic model (41), it is possible to choose the precoder $\tilde{\mathbf{C}}$ according to the optimality criterion specified in the following theorem.

Theorem 1 [11]: If $\mathbf{h}$ and $\tilde{\mathbf{w}}(i)$ in (41) are uncorrelated and $\tilde{\mathbf{w}}(i)$ is white, the optimum precoding matrix $\tilde{\mathbf{C}}$ is given by: $\tilde{\mathbf{C}}_{\rm opt} = \mathbf{\Phi}\mathbf{D}_f\mathbf{U}_h^{\mathcal{H}}$, where $\mathbf{U}_h$ is defined in (36); diagonal matrix $\mathbf{D}_f$ is the optimal power loading matrix selected as in [11, eqs. (17) and (18)], and $\mathbf{\Phi}$ an arbitrary $N \times (L+1)$ matrix with orthonormal columns. Optimality of $\tilde{\mathbf{C}}_{\rm opt}$ pertains to either minimizing the error in estimating the random channel, $E\{\|\mathbf{h} - \hat{\mathbf{h}}\|^2\}$, or, maximizing the conditional mutual information $I(\tilde{\mathbf{y}}(i), \mathbf{h}|s(i))$ if $\mathbf{h}$ is complex Gaussian distributed.

If the entries of $\mathbf{h}$ are independent and identically distributed (i.i.d.), i.e., $\mathbf{R}_{hh} = \sigma_h^2\mathbf{I}$ with $\mathbf{U}_h = \mathbf{I}_{L+1}$, then the optimal power loading matrix $\mathbf{D}_f = \alpha\mathbf{I}_{L+1}$, where $\alpha^2 = \mathcal{P}_0/(L+1)$[11]. In this case, the optimal precoder $\tilde{\mathbf{C}}_{\rm opt} = \alpha\mathbf{\Phi}$ should have orthogonal columns. Because the matrix $\mathbf{D}(\mathbf{c}_{\rm mc})\mathbf{V}$ has orthogonal columns while the Toeplitz matrix $\bar{\mathbf{C}}_{\rm ds}$ in general does not, MC-SS is optimal in this setting and it thus outperforms DS-SS with codes not having PACF.

The optimality in Theorem 1 amounts to minimizing the mean-square channel estimation error, which implies that

channel estimation accuracy dictates the overall BER performance. However, for special cases, it is possible to have the power loading of Theorem 1 optimize the overall BER directly (see, e.g., [3] for differential BPSK constellations which lead to a simple closed-form BER expression).

When the entries of $\mathbf{h}$ are i.i.d. with Gaussian distribution and covariance matrix $\mathbf{R}_{hh} = \sigma_h^2\mathbf{I}$, we next establish the optimality of MC-SS based on the SER expression in (39). Because $\mathbf{R}_{hh} = \sigma_h^2\mathbf{I}_{L+1}$, we have $\mathbf{D}_c$ in (37) for MC-SS as: $\mathbf{D}_c^{(\mathrm{mc})} = N\sigma_h^2\mathbf{I}_{L+1}$. Therefore, $\mathbf{D}_c^{(\mathrm{mc})}$ for MC-SS has equal diagonal entries, which is not the case for DS-SS because $\bar{\mathbf{C}}_{\mathrm{ds}}$ for DS-SS in (37) does not have orthogonal columns in general. However, the total transmitted power is the same because

$$\begin{aligned}\mathrm{tr}\left\{\mathbf{D}_c^{(\mathrm{ds})}\right\} &= \mathrm{tr}\left\{\bar{\mathbf{C}}_{\mathrm{ds}}\mathbf{R}_{hh}\bar{\mathbf{C}}_{\mathrm{ds}}^{\mathcal{H}}\right\} = \sigma_h^2\mathrm{tr}\left\{\bar{\mathbf{C}}_{\mathrm{ds}}^{\mathcal{H}}\bar{\mathbf{C}}_{\mathrm{ds}}\right\} \\ &= N(L+1)\sigma_h^2 = \mathrm{tr}\left\{\mathbf{D}_c^{(\mathrm{mc})}\right\}. \end{aligned} \tag{42}$$

Let us denote the ith diagonal element of $\mathbf{D}_c^{(\mathrm{ds})}$ by $\bar{\lambda}_{ii}^{(\mathrm{ds})}$ and of $\mathbf{D}_c^{(\mathrm{mc})}$ by $\bar{\lambda}_{ii}^{(\mathrm{mc})}$. We then have $\bar{\lambda}_{ii}^{(\mathrm{mc})} = \left(\sum_{i=1}^{L+1}\bar{\lambda}_{ii}^{(\mathrm{ds})}\right)/(L+1)$. Applying the inequality: $(x_1+x_2+\cdots+x_N) \geq N(x_1,x_2,\ldots,x_N)^{1/N}, x_i > 0$, we obtain $(x_1,x_2,\ldots,x_N)^{-1} \geq [(x_1+x_2+\cdots+x_N)/N]^{-N} \geq 0$, and after taking into account (40), we arrive at the following inequality:

$$\begin{aligned}\prod_{i=1}^{L+1} I_i\left(\frac{\bar{\lambda}_{ii}^{(\mathrm{ds})}\sigma_s^2}{\sigma_w^2}, \gamma_{\mathrm{PSK}}, \theta\right) &= \prod_{i=1}^{L+1}\left[1+\frac{\gamma_{\mathrm{PSK}}\bar{\lambda}_{ii}^{(\mathrm{ds})}\sigma_s^2}{\sigma_w^2\sin^2\theta}\right]^{-1} \\ &\geq \left[I_i\left(\frac{\bar{\lambda}_{ii}^{(\mathrm{mc})}\sigma_s^2}{\sigma_w^2}, \gamma_{\mathrm{PSK}}, \theta\right)\right]^{L+1}. \end{aligned} \tag{43}$$

Substituting (43) back into (39), we thus obtain

$$P_s^{(\mathrm{ds})}(E) \geq P_s^{(\mathrm{mc})}(E) \tag{44}$$

where equality is achieved when the Toeplitz matrix $\bar{\mathbf{C}}_{\mathrm{ds}}$ for DS-SS has orthogonal columns, i.e., when self-interference is zero. Inequality (43) implies that equal power loading optimizes SER for i.i.d. Gaussian channels. By distributing its power evenly across all subbands, MC-SS provides maximum protection against random frequency-selective multipath fading in this case.

If $\mathbf{h}$ is non i.i.d., equipower loading $\mathbf{D}_f = \alpha\mathbf{I}_{L+1}$ turns out to be near optimal at high SNR [11]. The selected precoder matrix $\check{\mathbf{C}} = \alpha\mathbf{\Phi}\mathbf{U}_h$ has orthogonal columns, which corroborates the near-optimality of MC-SS at high SNR.

To shed further light on the performance of digital MC-SS relative to DS-SS and to study the code dependence of DS-SS, we consider the following scenarios.

We construct three channel models, assuming that the channel $\mathbf{h}$ is Gaussian distributed of order $L = 2$. Channel 1 is i.i.d. with $\mathbf{R}_{hh} = \mathrm{diag}(1,1,1)/3$; channel 2 has $\mathbf{R}_{hh} = \mathrm{diag}(1,0.5,0.1)/1.6$, i.e., the first path shows a 3-dB gain over the second and 10-dB gain over the third path; and channel 3 is adopted from [3] with $\mathbf{R}_{hh} = \mathrm{diag}(1,0.05,0.01)/1.06$, i.e., the first path has a 13 dB gain over the second and 20 dB gain over the third path.

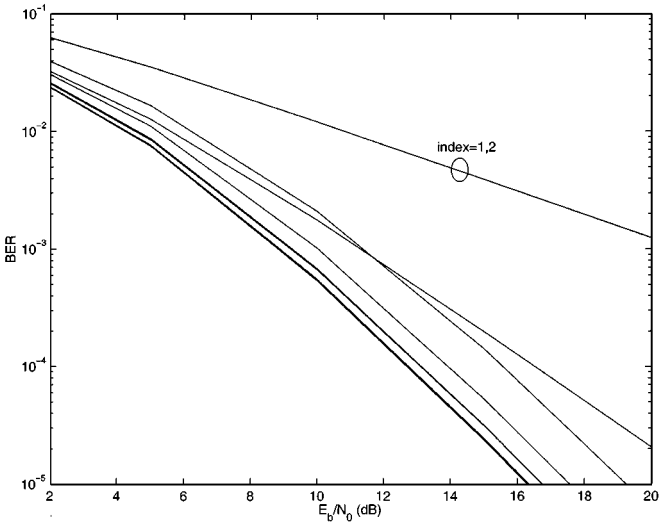

Fig. 7. DS-SS with different W–H codes of length $P = 16$. The channel has order $L = 2$, with i.i.d taps. This figure is to show the performance difference with different W–H codes.

Although we only illustrate channels with uncorrelated taps here, results can be easily extended to channels with correlated taps by decorrelating the channels first. Actually, channel 3 corresponds to a correlated channel with the same variance on each tap and correlation coefficients $\rho_{12} = \rho_{23} = 0.94$, and $\rho_{13} = 0.86$ [3].

With channel 1, Fig. 7 demonstrates the strong dependence of DS-SS on the code choices where different Walsh–Hadamard (W–H) codes of length $P = 16$ are used.[3] To avoid the code dependence, we again resort to code-hopping or long code spreading; the latter corresponds to using random spreading codes. For W–H codes, we discard the two bad codes which correspond to the first and second columns of a Hadamard matrix, because they lead to poor performance under multipath fading as confirmed by Fig. 7. It is known that W–H codes have poor autocorrelation properties. Therefore, we also employ Gold codes, which have better autocorrelation properties [21]. We adopt BPSK constellation. In Figs. 8–10, we compare the BER of MC-SS with the average BER of DS-SS with W–H codes and random codes of length $P = 8$, 16, 32, and with Gold codes of length $P = 7$, 15, 31, respectively. First, we see that MC-SS outperforms DS-SS with W–H codes considerably because the multipath induced self-interference of W–H codes is large. When Gold sequences or random codes are employed, we observe that the BER of DS-SS approaches that of MC-SS when the code length increases, as the self-interference becomes relatively smaller and smaller. In Fig. 8, note that MC-SS offers a 3–4-dB advantage over DS-SS at BER of 10^{-5}. Since Gold sequences and random codes offer almost the same performance, we omit the performance for random codes in the following.

With colored channels, we observe similar results as those in Figs. 8–10 for i.i.d channels. We compare in Fig. 11 MC-SS against DS-SS with code length 16 for both channels 2 and 3. Although MC-SS is not optimum (near optimum at high SNR)

[3]In Fig. 7 and thereafter, we define $E_b = N\sigma_s^2$ rather than $P\sigma_s^2$ by ignoring L guard chips. The power penalty $10\log(P/N)$ is negligible if $N \gg L$.

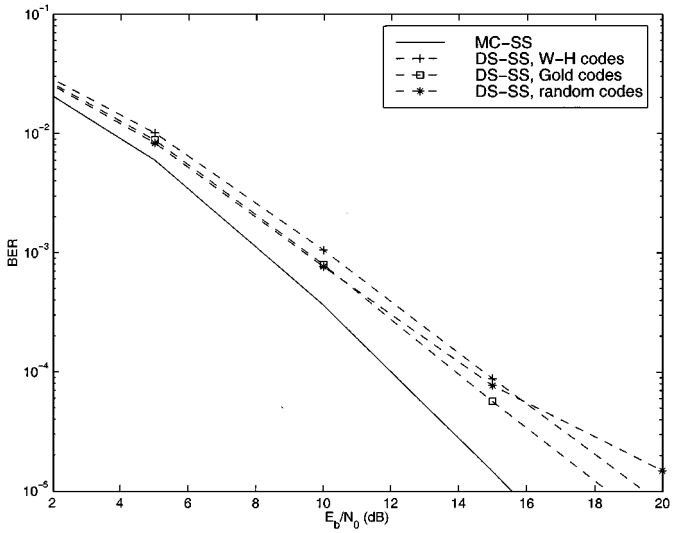

Fig. 8. MC-SS versus DS-SS with $P = 8$.

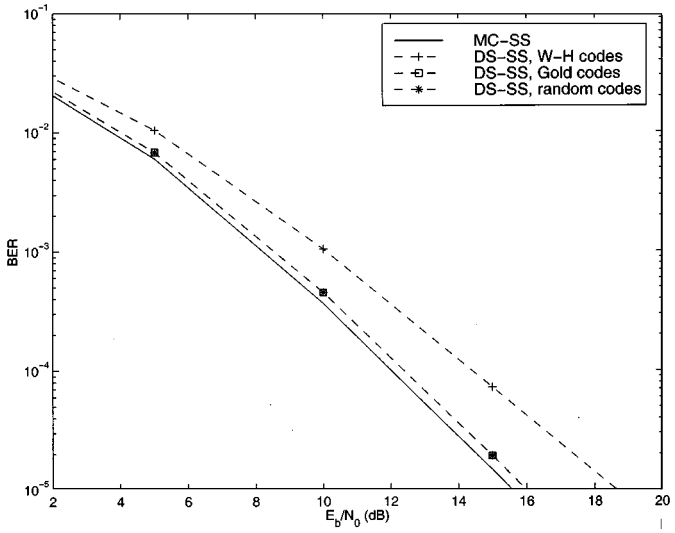

Fig. 9. MC-SS versus DS-SS with $P = 16$.

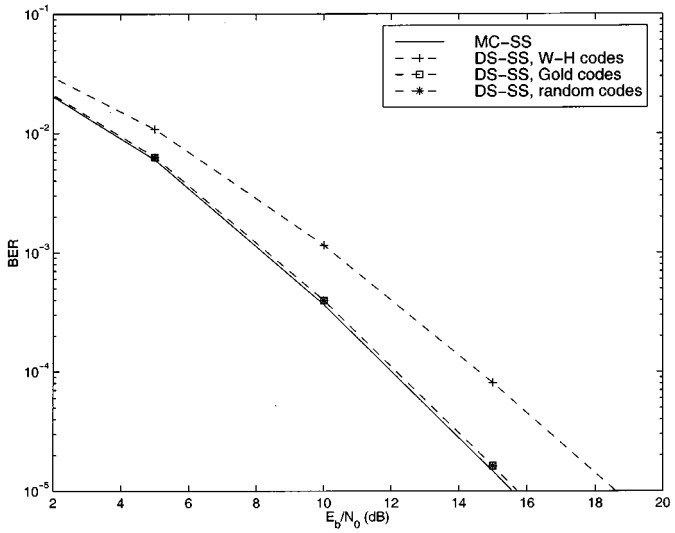

Fig. 10. MC-SS versus DS-SS with $P = 32$.

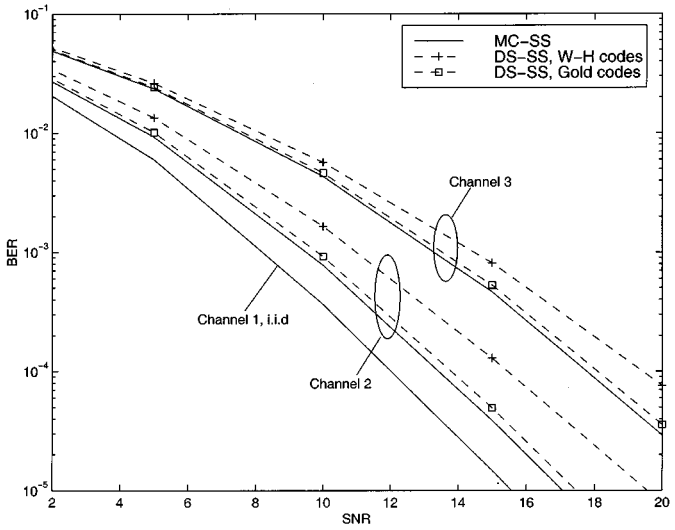

Fig. 11. MC-SS versus DS-SS, different multipath channels.

in these two channel settings, we clearly see that MC-SS outperforms DS-SS alternatives, especially when the spreading codes for DS-SS are not well constructed.

In this section, we focused on multipath effects, which destroy the orthogonality of codes. We used results from [11] for the optimal coding matrix, and showed that in the case of uncorrelated and equal power paths, the optimal code leads to MC-SS. If the codes in DS-SS are designed to have perfect PACF or have zero correlation zone with $L_{\mathrm{ZCZ}} \geq L$, DS-SS achieves the same performance as MC-SS. However, with widely used spreading codes, MC-SS outperforms DS-SS; with increasing spreading gain, the differences become less pronounced. In the case of colored channels (correlated paths and/or paths with unequal powers), MC-SS outperforms DS-SS in general, especially for short spreading lengths.

V. Multipath and NBI/PBI

In this section, we consider the general case where NBI/PBI is present and the channel is frequency selective. Starting from the general model (9), we assume that $\mathbf{c}$ and $\mathbf{w}$ are random vectors with covariance matrices $\mathbf{R}_{cc}$ and $\mathbf{R}_{ww}$, respectively. We then define

$$\mathbf{y}'(i) = \mathbf{R}_{ww}^{-1/2}\mathbf{y}(i) = \mathbf{R}_{ww}^{-1/2}\mathbf{c}s(i) + \mathbf{w}'(i) \tag{45}$$

where $\mathbf{w}'(i) := \mathbf{R}_{ww}^{-1/2}\mathbf{w}(i)$ is white with identity covariance matrix.

The MMSE estimator is: $\hat{s}(i) = \mathbf{g}_{\mathrm{mmse}}^{T}\mathbf{y}(i) = \mathbf{c}^{\mathcal{H}}\mathbf{R}_{ww}^{-1/2}\mathbf{y}'(i)$, which coincides with the MRC output operating on $\mathbf{y}'(i)$. Defining the equivalent code vector as $\mathbf{c}' := \mathbf{R}_{ww}^{-1/2}\mathbf{c}$, we reduce this colored problem to the white noise case discussed in Section IV. We can thus obtain closed-form SER expressions for this general case, by following similar steps.

Specifically, we decompose the equivalent covariance matrix $\mathbf{R}_{c'c'} := E\{\mathbf{c}'(\mathbf{c}')^{\mathcal{H}}\}$ as

$$\mathbf{R}_{c'c'} := \mathbf{R}_{ww}^{-1/2}\mathbf{R}_{cc}\mathbf{R}_{ww}^{-1/2} = \mathbf{U}_{c'}\mathbf{D}_{c'}\mathbf{U}_{c'}^{\mathcal{H}} \tag{46}$$

where $\mathbf{U}_{c'}$ is $N \times (L+1)$ unitary and $\mathbf{D}_{c'}$ is a diagonal matrix with diagonal entries $\lambda'_{ii}, i = 1, 2, \ldots, L+1$. The SER can

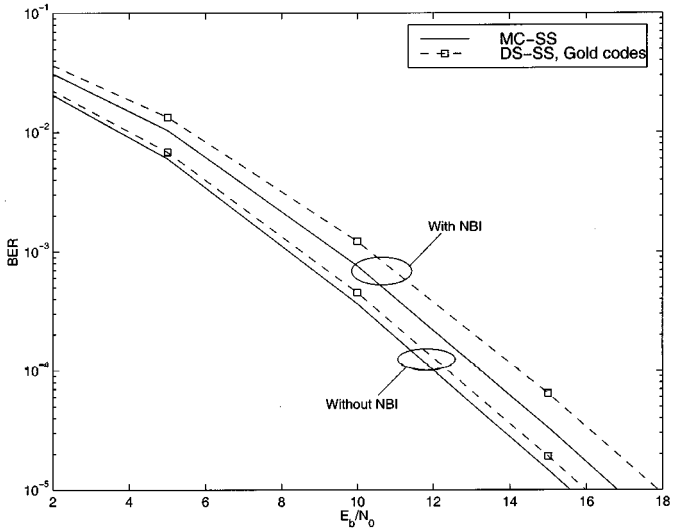

Fig. 12. MC-SS versus DS-SS, multipath plus NBI.

now be found from (39) after substituting $\bar{\lambda}_{ii}$ by λ'_{ii} and setting $\sigma_w^2 = 1$, i.e.,

$$P_s(E) = \frac{1}{\pi}\int_0^{(M-1)\pi/M} \prod_{i=1}^{L} I_i(\lambda'_{ii}\sigma_s^2, \gamma_{\rm PSK}, \theta)d\theta. \quad (47)$$

Note that this procedure is applicable to any type of interference provided that the covariance matrix $\mathbf{R}_{ww}$ (or a consistent estimate of it) is available.

Given the channel and noise covariance matrices $\mathbf{R}_{hh}$ and $\mathbf{R}_{ww}$, we can find $\mathbf{R}_{c'c'} = \mathbf{R}_{ww}^{-1/2}\bar{\mathbf{C}}_{\rm ds}\mathbf{R}_{hh}\bar{\mathbf{C}}_{\rm ds}^{\mathcal{H}}\mathbf{R}_{ww}^{-1/2}$ for DS-SS and $\mathbf{R}_{c'c'} = \mathbf{R}_{ww}^{-1/2}\mathbf{D}(\mathbf{c}_{\rm mc})\mathbf{V}\mathbf{R}_{hh}\mathbf{V}^{\mathcal{H}}\mathbf{D}(\mathbf{c}_{\rm mc}^{\mathcal{H}})\mathbf{R}_{ww}^{-1/2}$ for MC-SS. Recall that if As1) holds in MC-SS, then $\mathbf{R}_{c'c'} = \mathbf{D}(\mathbf{c}_{\rm mc})\mathbf{\Delta}^{-1/2}\mathbf{V}\mathbf{R}_{hh}\mathbf{V}^{\mathcal{H}}\mathbf{\Delta}^{-1/2}\mathbf{D}(\mathbf{c}_{\rm mc}^{\mathcal{H}})$ has the same eigenvalues as $\mathbf{\Delta}^{-1/2}\mathbf{V}\mathbf{R}_{hh}\mathbf{V}^{\mathcal{H}}\mathbf{\Delta}^{-1/2}$, since they are similar matrices. Therefore, the SER for MC-SS does not depend on code choices even in the joint presence of *both* multipath and NBI/PBI. The same argument holds true for cyclic prefixed transmission of DS-SS with CAZAC sequences, applying the same processing at the receiver.

Having compared DS-SS with MC-SS under NBI/PBI and multipath separately in Sections III and IV, we now test their performance in the joint presence of multipath and NBI/PBI via a simulation study. We use the same parameters as those leading to the results shown in Fig. 9 (i.i.d. channel 1 with Gold codes of length 15). Narrowband interference is now present in addition to multipath fading. We set the relative bandwidth of the NBI to $\epsilon = 3/16$, and the PSD ratio relative to the background noise as $10\log_{10}(J_0/N_0) = 13$ dB. Fig. 12 shows that the BER for MC-SS is lower than the average BER of DS-SS with Gold sequences. Relative to the case without NBI/PBI, the gap between MC-SS and DS-SS increases when NBI/PBI is present as shown in Fig. 12, which corroborates the robustness of MC-SS (relative to DS-SS) with respect to frequency-selective multipath fading and narrow (or partial) band interference.

In this section, we compared MC-SS with DS-SS in the presence of both NBI/PBI and multipath fading. A closed-form expression for the SER was derived; it was seen that the SER for MC-SS is independent of the code in this case as well. Again, DS-SS can have the same performance as MC-SS with codes having perfect PACF. We showed via simulations that MC-SS outperforms DS-SS when degradations occur due to both multipath fading and NBI/PBI, if the codes in DS-SS do not possess perfect PACF.

VI. Discussion and Conclusions

Our previous observations illustrate that: in order to improve the system performance, DS-SS systems need to adopt codes with flat spectra to cope with NBI, and with good autocorrelation properties to cope with multipath. It is established in Lemma 1 that a code with flat spectrum has perfect PACF, and vice versa. Relaxing the constraint that the spreading codes in DS-SS should have unit amplitude, we can actually view MC-SS as a cyclic prefixed transmission of DS-SS, but with an equivalent nonconstant-amplitude spreading code $\bar{\mathbf{c}}_{\rm mc} = \mathbf{F}_N^{\mathcal{H}}\mathbf{c}_{\rm mc}$. Since $\mathbf{F}_N\bar{\mathbf{c}}_{\rm mc} = \mathbf{c}_{\rm mc}$ has unit-amplitude entries, this equivalent code $\bar{\mathbf{c}}_{\rm mc}$ has flat spectrum. Using Lemma 1, $\bar{\mathbf{c}}_{\rm mc}$ thus has perfect PACF (notice that Lemma 1 applies to any code sequence). Therefore, the improvement of MC-SS over DS-SS with conventional constant-amplitude spreading codes is precisely due to an underlying construction of an equivalent code having nonconstant amplitude but possessing perfect PACF. Instead of redesigning new spreading codes with both constant amplitude and perfect PACF, MC-SS simply constructs equivalent codes by taking the IFFT of conventional spreading codes. The price paid is certainly nonconstant modulus transmissions, which limits the power-efficiency of the amplifier.

Our focus in this paper was on the single user case. In multiuser systems, our conclusions hold true *only if* multiuser interference (MUI) can be modeled as additive Gaussian noise, e.g., in a moderate to high loaded asynchronous CDMA system with long (random) code spreading (see also [16] and [19] for the Gaussian approximation). The practical cases, where the number of users is not large and Gaussian modeling becomes inappropriate, need further investigation. Nevertheless, the single user performance can serve as a bound for multiuser systems assuming that the contribution of MUI can be perfectly estimated and subtracted. On the other hand, since MUI is eliminated deterministically rather than statistically, generalized multi-carrier CDMA appropriate for the multiple access scenario can be developed, and will be reported elsewhere (some preliminary results may be found in [28]).

In a nutshell, we developed closed-form expressions for the symbol error rate (SER) of digital multi-carrier spread-spectrum (MC-SS) modulation; we then compared MC-SS with direct-sequence spread spectrum (DS-SS) under different scenarios: AWGN channel with narrow/partial band interference (NBI/PBI), and frequency-selective multipaths with or without NBI/PBI. The performance of MC-SS does not depend upon the spreading code; in contrast, the performance of DS-SS does depend upon the spreading code. For carefully designed spreading codes with perfect periodic auto correlation function (PACF), DS-SS (with cyclic prefixed transmission) achieves the same performance as MC-SS. For widely used spreading sequences that do not have perfect PACF, we showed that MC-SS with symbol periodic codes outperforms DS-SS with

long codes or code hopping, while the performance difference decreases as the spreading gain increases. The improvement of MC-SS over DS-SS stems precisely from the underlying step relaxing the constant amplitude requirement on the DS-SS code to construct an equivalent nonconstant-amplitude code with perfect periodic autocorrelation. The extension to multiuser systems is under current investigation.

APPENDIX
PROOF OF $\mathrm{tr}\{\mathbf{\Delta}\}\mathrm{tr}\{\mathbf{\Delta}^{-1}\} \geq N^2$

Because $\mathbf{\Delta}$ is a diagonal matrix, we have $\mathrm{tr}\{\mathbf{\Delta}\} = \sum_{i=1}^{N} \delta_{ii}$ and $\mathrm{tr}\{\mathbf{\Delta}^{-1}\} = \sum_{i=1}^{N} 1/\delta_{ii}$. Since $\delta_{ii} > 0,\ \forall\, i \in [1, N]$, we can apply the inequalities

$$\sum_{i=1}^{N} \delta_{ii} \geq N\left(\prod_{i=1}^{N} \delta_{ii}\right)^{1/N}, \quad \sum_{i=1}^{N} \frac{1}{\delta_{ii}} \geq N\left(\prod_{i=1}^{N} \frac{1}{\delta_{ii}}\right)^{1/N}$$

to obtain $\mathrm{tr}\{\mathbf{\Delta}\}\mathrm{tr}\{\mathbf{\Delta}^{-1}\} \geq N^2$.

ACKNOWLEDGMENT

The authors would like to thank Prof. M.-S. Alouini from the Electrical and Computer Engineering Department at the University of Minnesota for pointing their attention to [3] and [25]. The authors are grateful to one of the anonymous reviewers for suggesting the CAZAC sequences of [6] and [9].

REFERENCES

[1] J. A. C. Bingham, "Multicarrier modulation for data transmission: An idea whose time has come," *IEEE Commun. Mag.*, pp. 5–14, May 1990.
[2] D. R. Brillinger, *Time Series: Data Analysis and Theory*. San Francisco, CA: Holden-Day, 1981.
[3] J. K. Cavers, "Optimized use of diversity modes in transmitter diversity systems," in *Proc. IEEE Vehicular Technology Conf.*, vol. 3, 1999, pp. 1768–1773.
[4] J. S. Cha, S. Kameda, M. Yokoyama, H. Nakase, K. Masu, and K. Tsubouchi, "New binary sequences with zero-correlation duration for approximately synchronized CDMA," *Electron. Lett.*, vol. 36, no. 11, pp. 991–993, May 2000.
[5] K. Cheun, K. Choi, H. Lim, and K. Lee, "Anti-jamming performance of a multicarrier direct-sequence spread-spectrum system," *IEEE Trans. Commun.*, vol. 47, pp. 1781–1784, Dec. 1999.
[6] D. C. Chu, "Polyphase codes with good periodic correlation properties," *IEEE Trans. Inform. Theory*, vol. 18, pp. 531–532, July 1972.
[7] T. M. Cover and J. A. Thomas, *Elements of Information Theory*. New York: Wiley, 1991.
[8] X. Deng and P. Fan, "Spreading sequence sets with zero correlation zone," *Electron. Lett.*, vol. 36, no. 11, pp. 993–994, May 2000.
[9] R. L. Frank and S. A. Zadoff, "Phase shift pulse codes with good periodic correlation properties," *IRE Trans. Inform. Theory*, vol. 8, pp. 381–382, Oct. 1962.
[10] G. B. Giannakis, P. Anghel, and Z. Wang, "Wideband generalized multicarrier CDMA over frequency-selective wireless channels," in *Proc. Int. Conf. on Acoustics, Speech, and Signal Processing*, Istanbul, Turkey, June 5–9, 2000, pp. 2501–2504.
[11] G. B. Giannakis and S. Zhou, "Optimal transmit-diversity precoders for random fading channels," in *Proc. Globecom Conf.*, vol. 3, San Francisco, CA, Dec. 1, 2000, pp. 1839–1843.
[12] S. Haykin, *Adaptive Filter Theory*, 3rd ed. Englewood Cliffs, NJ: Prentice Hall, 1996.
[13] R. C. Heimiller, "Phase shift pulse codes with good periodic correlation properties," *IRE Trans. Inform. Theory*, vol. 7, no. 4, pp. 254–257, Oct. 1961.
[14] G. K. Kaleh, "Frequency-diversity spread-spectrum communication system to counter bandlimited Gaussian interference," *IEEE Trans. Commun.*, vol. 44, pp. 886–893, July 1996.
[15] S. M. Kay, *Fundamentals of Statistical Signal Processing, Volume II: Detection Theory*. Englewood Cliffs, NJ: Prentice-Hall, 1998.
[16] S. Kondo and L. B. Milstein, "Performance of multicarrier DS CDMA systems," *IEEE Trans. Commun.*, vol. 44, pp. 238–46, Feb. 1996.
[17] L. B. Milstein, D. L. Schilling, R. L. Pickholtz, V. Erceg, M. Kullback, E. G. Kanterakis, D. S. Fishman, W. H. Biederman, and D. C. Salerno, "On the feasibility of a CDMA overlay for personal communications networks," *IEEE J. Select. Areas Commun.*, vol. 10, pp. 655–668, May 1992.
[18] C. L. Ng, K. B. Letaief, and R. D. Murch, "Complex optimal sequences with constant magnitude for fast channel estimation initialization," *IEEE Trans. Commun.*, vol. 46, pp. 305–308, Mar. 1998.
[19] E. Papproth and G. K. Kaleh, "A CDMA overlay system using frequency-diversity spread spectrum," *IEEE Trans. Veh. Technol.*, vol. 48, pp. 397–404, Mar. 1999.
[20] S. Parkvall, "Variability of user performance in cellular DS-CDMA—Long versus short spreading sequences," *IEEE Trans. Commun.*, vol. 48, pp. 1178–1187, July 2000.
[21] J. Proakis, *Digital Communications*, 3rd ed. New York: McGraw-Hill, 1995.
[22] U. H. Rohrs and L. P. Linde, "Some unique properties and applications of perfect squares minimum phase CAZAC sequences," in *Proc. South African Symp. on Communications and Signal Processing*, 1992, pp. 155–160.
[23] G. J. Saulnier, M. Mettke, and M. J. Medley, "Performance of an OFDM spread spectrum communication system using lapped transforms," in *Proc. MILCOM Conf.*, 1997, pp. 608–612.
[24] G. J. Saulnier, Z. Ye, and M. J. Medley, "Performance of a spread spectrum OFDM system in a dispersive fading channel with interference," in *Proc. MILCOM Conf.*, 1998, pp. 679–683.
[25] M. K. Simon and M.-S. Alouini, "A unified approach to the performance analysis of digital communication over generalized fading channels," *Proc. IEEE*, vol. 86, pp. 1860–1877, Sept. 1998.
[26] Z. Wang and G. B. Giannakis, "Wireless multicarrier communications: Where fourier meets Shannon," *IEEE Signal Processing Mag.*, pp. 29–48, May 2000.
[27] N. Yee, J.-P. Linnartz, and G. Fettweis, "Multicarrier CDMA in indoor wireless radio networks," in *Proc. IEEE PIMRC*, Sept. 1993, pp. 109–113.
[28] S. Zhou, G. B. Giannakis, and A. Swami, "Frequency-hopped generalized MC-CDMA for multipath and interference suppression," in *Proc. MILCOM Conf.*, vol. 2, Los Angeles, CA, Oct. 22–25, 2000, pp. 937–941.
[29] R. L. Peterson, R. E. Ziemer, and D. E. Borth, *Introduction to Spread Spectrum Communications*. Englewood Cliffs, NJ: Prentice-Hall, 1995.

Shengli Zhou (S'99) was born in Anhui, China, in 1974. He received the B.S. and M.Sc. degrees from the University of Science and Technology of China (USTC), both in electrical engineering and information science, in 1995 and 1998, respectively. He is currently working toward the Ph.D. degree in the Department of Electrical and Computer Engineering, University of Minnesota, Minneapolis.

His broad interests lie in the areas of communications and signal processing, including transceiver optimization, blind channel estimation and equalization algorithms, wireless, multi-carrier, space-time coded and spread-spectrum communication systems.

Georgios B. Giannakis (F'97) received his Diploma in Electrical Engineering from the National Technical University of Athens, Greece, in 1981 and the M.S.c. degree in electrical engineering, the M.Sc. degree in mathematics, and the Ph.D. degree in electrical engineering from the University of Southern California (USC), in 1983, 1986, and 1986, respectively.

After lecturing for one year at USC, he joined the University of Virginia in 1987, where he became a professor of Electrical Engineering in 1997. Since 1999 he has been a professor with the Department of Electrical and Computer Engineering at the University of Minnesota, where he now holds an ADC Chair in Wireless Telecommunications. His general interests span the areas of communications and signal processing, estimation and detection theory, time-series analysis, and system identification—subjects on which he has published more than 140 journal papers, 270 conference papers and two edited books. Current research topics focus on transmitter and receiver diversity techniques for single- and multi-user fading communication channels, redundant precoding and space-time coding for block transmissions, multicarrier, and wide-band wireless communication systems.

Dr. Giannakis is the co-recipient of four best paper awards from the IEEE Signal Processing (SP) Society (1992, 1998, 2000, and 2001). He has also received the Society's Technical Achievement Award in 2000. He co-organized three IEEE-SP Workshops (HOS in 1993, SSAP in 1996 and SPAWC in 1997) and co-guest edited four special issues. He has served as an Associate Editor for the IEEE TRANSACTIONS ON SIGNAL PROCESSING and the IEEE SIGNAL PROCESSING LETTERS. He is a secretary of the IEEE SP Conference Board, a member of the IEEE SP Publications Board and a member and vice-chair of the Statistical Signal and Array Processing Committee. He is a member of the Editorial Board for the PROCEEDINGS OF THE IEEE, he chairs the SP for Communications Technical Committee and serves as the Editor in Chief for the IEEE SIGNAL PROCESSING LETTERS. He is a member of the IEEE Fellows Election Committee, the IEEE-SP Society's Board of Governors, and a frequent consultant for the telecommunications industry.

Ananthram Swami (SM'96) received the B.S. degree from the Indian Institute of Technology, Bombay, India, the M.S. degree from Rice University, Houston, TX, and the Ph.D. degree from the University of Southern California, Los Angeles, all in electrical engineering.

He has held positions with Unocal Corporation, the University of Southern California, CS-3, and Malgudi Systems. He is currently a Research Scientist with the Communication Networks Branch of the Army Research Laboratory, Adelphi, MD, where his work is in the broad area of signal processing for communications. He was a Statistical Consultant to the California Lottery, developed a Matlab-based toolbox for non-Gaussian signal processing, and has held visiting faculty positions at INP, Toulouse, France. He has taught short courses for industry, and currently teaches courses on communication theory and signal processing at the University of Maryland.

Dr. Swami is a member of the IEEE Signal Processing Society's (SPS) technical committee (TC) on Signal Processing for Communications, a member of the IEEE Communication Society's TC on Tactical Communications, and an Associate Editor for IEEE SIGNAL PROCESSING LETTERS. He was a member of the society's TC on Statistical Signal and Array Processing (1993–98); an Associate Editor of the IEEE TRANSACTIONS ON SIGNAL PROCESSING; and co-organizer and co-chair of the 1993 IEEE SPS Workshop on Higher-Order Statistics, the 1996 IEEE SPS Workshop on Statistical Signal and Array Processing, and the 1999 ASA-IMA Workshop on Heavy-Tailed Phenomena.